Off-shell single-top production at NLO matched to parton showers

R. Frederix,[a] **S. Frixione,**[b] **A.S. Papanastasiou,**[c] **S. Prestel**[d] **and P. Torrielli**[e]

[a]*Physik Department T31, Technische Universität München,*
James-Franck-Str. 1, D-85748 Garching, Germany

[b]*INFN — Sezione di Genova,*
Via Dodecaneso 33, I-16146, Genoa, Italy

[c]*Cavendish Laboratory, University of Cambridge,*
J.J. Thomson Avenue, CB3 0HE, Cambridge, U.K.

[d]*SLAC National Accelerator Laboratory,*
2575 Sand Hill Road, Menlo Park, CA 94025-7090 U.S.A.

[e]*Dipartimento di Fisica, Università di Torino and INFN — Sezione di Torino,*
Via P. Giuria 1, I-10125, Turin, Italy

E-mail: rikkert.frederix@tum.de, Stefano.Frixione@cern.ch,
andrewp@hep.phy.cam.ac.uk, prestel@slac.standford.edu,
torriell@to.infn.it

ABSTRACT: We study the hadroproduction of a Wb pair in association with a light jet, focusing on the dominant t-channel contribution and including exactly at the matrix-element level all non-resonant and off-shell effects induced by the finite top-quark width. Our simulations are accurate to the next-to-leading order in QCD, and are matched to the HERWIG6 and PYTHIA8 parton showers through the MC@NLO method. We present phenomenological results relevant to the 8 TeV LHC, and carry out a thorough comparison to the case of on-shell t-channel single-top production. We formulate our approach so that it can be applied to the general case of matrix elements that feature coloured intermediate resonances and are matched to parton showers.

KEYWORDS: NLO Computations, QCD Phenomenology

Contents

1 Introduction

Single-top production at hadron colliders has continued to be an active field of research, challenging both experimental and theoretical communities, since its observation at the Tevatron [1, 2]. Measurements of the dominant t-channel subprocess have been presented by CDF and D0 [3–5] at the Tevatron, as well as by the ATLAS [6–8] and CMS [9–11] collaborations, at both the 7 TeV and 8 TeV LHC, with preliminary results [12, 13] available at 13 TeV as well. This channel has also been exploited by the ATLAS collaboration in the first top-mass extraction from single-top events in ref. [14]. More recently, experimental evidence has been found [15–18] of s- and Wt-channel production, which are characterised by cross sections smaller than that of the t channel. Single top production has been shown to be sensitive to anomalous tWb-couplings (see for example refs. [19, 20]), and efforts are being made by experiments [21, 22] to use the t-channel process to search for such features. Furthermore, with increased statistics at run II of the LHC, measurements of the top-quark decay products and of differential quantities will be possible with vastly improved precision.

With a view to matching the progress achieved on the experimental side, it is important to review, assess and improve the current theoretical predictions available for single-top

production. Top quarks are never observed as stable particles, but rather their production is inferred through a kinematic reconstruction of their decay products (jets, leptons and missing energy). Theoretical predictions, whenever possible, should therefore reflect this fact, namely they should deal with top decay products instead of stable top quarks as primary objects. This is particularly important for observables sensitive to the decay and off-shellness of the top, as well as for those sensitive to non-resonant contributions, which are completely missing in the stable-top approximation.

Nonetheless, the current theoretical standard only partially fulfils this requirement. State-of-the-art predictions at the hadron level for this process are obtained through NLO-matching with parton showers (NLO+PS) both in the four- and five-flavour schemes [23–25] in the MC@NLO [26] and POWHEG [27, 28] approaches, assuming stable-top hard matrix elements. In such setups, the top-quark decay is performed with LO accuracy, and the off-shellness of the top propagator is introduced through a simple Breit-Wigner smearing, either by the PS itself, or at the matrix-element level (which allows one to correctly account for both production and decay spin correlations) by applying the method introduced in ref. [29]. At fixed order (where the most advanced predictions for the stable-top t-channel cross section are the NNLO results of ref. [30]), alongside the NLO corrections to the production, NLO corrections to the decay of the top quark have been included in the narrow-width approximation (NWA) [31–34]. A systematic treatment of off-shell effects for resonant top quarks was first presented in refs. [35, 36], using an effective-theory-inspired generalisation of the pole expansion. The NLO corrections to the t-channel process with full off-shell and non-resonant effects have been computed in ref. [37] by adopting the complex-mass scheme (CMS) [38, 39].

Including NLO QCD corrections to the top decay has been shown to play a significant role, especially for observables such as transverse momentum of the b-jet or the invariant mass of the lepton+b-jet system [34, 40]. Additionally, treating the top quark as on-shell (as in the NWA) or off-shell can also lead to striking differences in the NLO predictions of experimentally relevant observables [35–37], a prime example being the invariant mass of the reconstructed top (see also refs. [41–43] for similar features in $t\bar{t}$ production). In light of these observations at fixed order, understanding to what extent these effects survive the showering and hadronisation stages in a Monte Carlo (MC) is not only interesting from the theory point of view, but it also becomes crucial for improved predictions of the observables mentioned above. In particular, with predictions at NLO+PS accuracy and full off-shell effects at the hard matrix-element level, it becomes possible to validate NLO+PS approaches where the underlying hard matrix elements are computed in the on-shell-top approximation. It is also of great relevance to use these improved predictions to properly assess the systematics affecting the extraction of the top mass when using, as is currently done, MCs within which the hard matrix elements do not include full NLO off-shell effects. Recently, work has been performed in this direction in refs. [44, 45] within the POWHEG+Pythia8 framework, including NLO corrections in both production and decay, and considering $t\bar{t}$ production in the NWA and single-top t-channel production with full off-shell effects, respectively.

In this work we adopt the MC@NLO scheme, and study the NLO matching to parton showers of t-channel single-top hadroproduction with full off-shell and non-resonant effects,

namely the t-channel contribution to the EW process $pp \to W^+ b j$, with j being a light jet, at the 8 TeV LHC. We match our computations to the HERWIG6 [46, 47] and PYTHIA8 [48] parton showers. In this context, we discuss in general the subtleties that occur in NLO+PS simulations for processes with intermediate coloured resonances, and perform a thorough comparison to other available approximations of t-channel single-top cross section. In doing so, we present a study of hadron-level observables sensitive to top-decay radiative corrections and off-shell effects. The shape of such observables is often a result of a sensitive interplay of a number of different phenomena, which we endeavour to disentangle and understand here.

We perform our calculations in the framework of MADGRAPH5_AMC@NLO [49], which automates all ingredients relevant to the simulation of LO and NLO cross sections, including the matching to parton showers. The FKS method [50, 51] (automated in the module MADFKS [52]) for the subtraction of the infrared (IR) singularities of real-emission matrix elements underpins all NLO-accurate results. The computations of one-loop amplitudes are carried out by switching dynamically between two integral-reduction techniques, OPP [53] and TIR [54–56]. These have been automated in the module MADLOOP [57], which in turn exploits CUTTOOLS [58] together with an in-house implementation of the OPENLOOPS optimisation [59]. Matching to parton showers is achieved by means of the MC@NLO formalism [26].

The paper is structured as follows: in section 2 we describe the setup of the computation, and in particular the subtleties related to the phase-space parametrisation, integration, and MC@NLO-type matching of processes with intermediate coloured resonances; in section 3 we discuss some details of the various approximations to the complete $W^+ b j$ process, and we present our results for a selected set of observables; in section 4 we draw our conclusions.

2 Matching setup, subtleties and technicalities

2.1 Integration of subtracted cross sections with resonances

Regardless of whether a computation that features an unstable intermediate particle (that henceforth we denote by β, and assume to have mass m_β and width $\Gamma_\beta \ll m_\beta$) is matched to parton showers, one problem which must be addressed is that of the efficient integration of the corresponding matrix elements. This is particularly non-trivial in the case where these matrix elements enter the real-emission contribution to an NLO cross section, owing to the necessity of IR-subtracting them. At the amplitude level, the unstable particle is represented by (at least) an s-channel propagator and thus the squared matrix elements will contain a term

$$\frac{1}{(k_\beta^2 - m_\beta^2)^2 + (\Gamma_\beta m_\beta)^2} \,, \tag{2.1}$$

with $k_\beta^2 > 0$ the virtuality of β. Because of eq. (2.1), kinematic configurations with $k_\beta^2 \simeq m_\beta^2$ will be associated with large weights, and hence the corresponding unweighted events will be more likely to occur. The likelihood of this increases with decreasing Γ_β, which is easy to understand also in view of the fact that the $\Gamma_\beta \to 0$ limit of eq. (2.1) is proportional to the

Dirac delta function $\delta(k_\beta^2 - m_\beta^2)$, that forces $k_\beta^2 = m_\beta^2$ exactly. An efficient matrix element integration therefore requires that the phase-space generation be biased towards $k_\beta^2 \simeq m_\beta^2$ configurations, a requirement which is independent of the perturbative order. At the LO (i.e. tree) level, this is not difficult to achieve. The most direct way is that of choosing k_β^2 as one of the integration variables, so that the adaptive integration quickly knows where to throw most of the phase-space points. This is what is done in MADGRAPH5_AMC@NLO. While one would like to apply a similar strategy at the NLO and beyond, it is the IR subtractions relevant to the real-emission terms that prevent one from doing this in a straightforward manner. In contrast, all of the other non-subtracted contributions to an NLO cross section, such as the Born and the virtuals, can be dealt with in exactly the same way as the LO. In order to simplify the discussion of the relevant issues without loss of generality, let us assume that only one type of singularity is relevant (say, the soft singularities). Following FKS, we shall denote by ξ the phase-space variable that in the limit $\xi \to 0$ causes the matrix elements to be soft-singular, and by b all of the other (Born-level) phase-space variables. The typical structure of the integrated NLO cross section will thus be:

$$\int db\, d\xi \frac{1}{\xi} \left[\varsigma\big(k_\beta^2(b,\xi)\,|\,b,\xi\big) - \varsigma\big(k_\beta^2(b,0)\,|\,b,0\big) \right],\tag{2.2}$$

where the redundant first argument (k_β^2) of the integrand ς (ς is equal to the matrix elements times phase-space factors) has been inserted explicitly only in view of its relevance to the present discussion. Because of the way eq. (2.2) is integrated (i.e. by choosing some b and ξ for any given random number), its event and counterevent contributions (first and second term, respectively, under the integral sign in eq. (2.2)) will typically have very different weights, owing to eq. (2.1), *unless* the condition

$$k_\beta^2(b,\xi) = k_\beta^2(b,0), \qquad \forall\, \xi, \quad b \text{ given}\tag{2.3}$$

is fulfilled. Such a difference in weights is responsible for a poorly-convergent integration.

In principle, this is simply an efficiency problem, since the convergence in the large-statistics limit is guaranteed by the condition

$$\lim_{\xi \to 0} k_\beta^2(b,\xi) = k_\beta^2(b,0),\tag{2.4}$$

which holds regardless of whether eq. (2.3) is true or not. In practice, however, the statistics one needs to accumulate rapidly grows with the inverse of Γ_β, becoming infinite in the $\Gamma_\beta \to 0$ limit. Indeed, it is instructive to consider the situation in the limiting case where eq. (2.1) is replaced by a Dirac delta. When this happens and the condition of eq. (2.3) is not fulfilled, then for any given b either the event or the counterevent is non-null, but never both simultaneously (since it is either $k_\beta^2(b,\xi) = m_\beta^2$ or $k_\beta^2(b,0) = m_\beta^2$). This implies that the phase space is partitioned into two disjoint regions, in which either only the event or only the counterevent contribution to the integrand of eq. (2.2) is non-null, which in turn renders the numerical integration impossible with finite statistics. Alternatively, and from a more physical viewpoint, in processes where Γ_β is very small, for the majority of phase-space points the event is computed at the resonance peak, while the counterevents

are far away from the peak (or vice versa), even though the energy of the emitted parton (ξ in eq. (2.2)) might be small as well. Thus, a small-width resonance severely hampers the cancellation between event and counterevents. A viable solution stems from a re-mapping of the phase space:

$$b \longrightarrow \Phi_\xi(b) \,. \tag{2.5}$$

There is ample freedom in choosing the specific form of eq. (2.5), but nevertheless we can distinguish two classes of re-mappings. The members of the first class fulfill the following condition:

$$k_\beta^2(b, \xi) = k_\beta^2(\Phi_\xi(b), 0) \,, \qquad \forall \xi \,, \tag{2.6}$$

for any given b. This can be exploited by rewriting eq. (2.2) as follows:

$$\int db\, d\xi \frac{1}{\xi} \left[\varsigma\big(k_\beta^2(b, \xi) \,|\, b, \xi\big) - \frac{\partial \Phi_\xi(b)}{\partial b} \varsigma\big(k_\beta^2(\Phi_\xi(b), 0) \,|\, \Phi_\xi(b), 0\big) \right] \,. \tag{2.7}$$

In other words, eq. (2.5) is used for changing the integration variables of the counterevent (see appendix A for a few technical details on this procedure). Thanks to this, the virtuality of β is the same in the event and counterevent of eq. (2.7), hence solving the original problem. Conversely, the re-mappings that belong to the second class fulfill the condition:

$$k_\beta^2(\Phi_\xi(b), \xi) = k_\beta^2(b, 0) \,, \qquad \forall \xi \,, \tag{2.8}$$

for any given b. One thus changes the integration variables of the event contribution, whence the analogous of eq. (2.7) reads:

$$\int db\, d\xi \frac{1}{\xi} \left[\frac{\partial \Phi_\xi(b)}{\partial b} \varsigma\big(k_\beta^2(\Phi_\xi(b), \xi) \,|\, \Phi_\xi(b), \xi\big) - \varsigma\big(k_\beta^2(b, 0) \,|\, b, 0\big) \right] \,, \tag{2.9}$$

which again solves the problem.

In summary, there are three possible ways out. The first, which we call a type-I solution, is that of choosing a phase-space parametrisation such that eq. (2.3) is fulfilled (this is essentially what has been done in ref. [45]). The second (called type-IIa solution) entails a re-mapping of the phase-space variables relevant to the counterevent, so that eq. (2.6) is fulfilled. Finally, with a type-IIb solution the re-mapping acts on the variables relevant to the event, so that eq. (2.8) is fulfilled. While approaches of type I are simpler than those of type II, they are not necessarily more convenient in the context of NLO or NLO+PS computations, where the primary concern is that of finding a phase-space parametrisation which is ideally suited to IR subtractions (and, in the case of NLO+PS, to MC matching). The latter requirement might render eq. (2.3) (and thus the direct application of the method of ref. [45]) difficult to achieve. It also implies that it is hard to find a solution to the problem which can be applied to a generic IR-subtraction formalism. It is much more convenient to work in the context of a specific subtraction scheme, and for this reason in what follows we shall concentrate on FKS and on its implementation in MadGraph5_aMC@NLO.
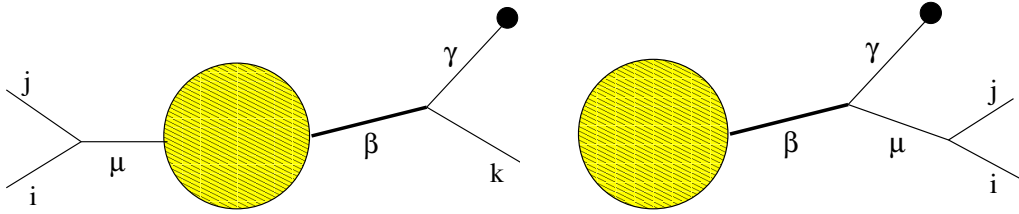
Figure 1. Left panel: the FKS pair (i, j) is not connected to the resonance β. Right panel: the FKS pair is connected to the resonance.

2.1.1 Treatment of resonances in FKS

We assume that the reader is familiar with the basics of FKS subtraction; if not, all of the relevant information can be found in the original papers [50, 51] and in ref. [52]. The latter work deals specifically with the issues relevant to automation, and hence to the MADGRAPH5_AMC@NLO implementation. There are two possible situations, depicted in figure 1: the case where the FKS pair — identified in what follows by the indices i (the FKS parton) and j (its sister) — is not directly connected to the tree[1] that stems from the resonance β (left panel); and the case where the FKS pair is part of the tree whose root is β (right panel). We also have to keep in mind that, at variance with the simplified treatment presented in section 2.1, in QCD there are both soft and collinear singularities. However, one of the key properties of the phase-space parametrisations relevant to FKS in MADGRAPH5_AMC@NLO is that for a given real-emission resolved configuration, the reduced (i.e. Born-like) configurations associated with the soft and collinear limits are identical to each other. We observe that this is a sufficient condition for a type-IIb approach to work (since the re-mapping of eq. (2.8) requires that the r.h.s. of that equation be unique for a given b). Conversely, type-IIa solutions might be implemented in any case, however with possibly different re-mappings associated with soft and collinear configurations.

The situation depicted in the left panel of figure 1 can occur with either initial-state or final-state singularities, and the phase-space parametrisation in MADGRAPH5_AMC@NLO offers a type-I solution in this case. This is because for both types of singularities all of the final-state momenta relevant to a given event (excluding i and j in the case of a final-state singularities) are related to those of the associated counterevents by means of boosts. Since neither i nor j contribute to the invariant mass of β, this implies that eq. (2.3) is fulfilled, and therefore one can choose k_β^2 as an integration variable.

Let us now turn to the situation depicted in the right panel of figure 1, which occurs solely in the case of final-state singularities. Relevant cases are for example that of a Z branching, with $(\beta, \mu, \gamma) = (Z, q, \bar{q})$ and $(i, j) = (g, q)$, or that of a top-quark branching, with $(\beta, \mu, \gamma) = (t, b, W)$ and $(i, j) = (g, b)$. In the current version of MAD-GRAPH5_AMC@NLO, the phase-space parametrisation adopted is that of section 5.2 of ref. [28], and its generalisation to the case of a massive FKS sister. Such a parametrisation

---

[1]Note that this is a sensible definition, because β is an s-channel, and hence it is the root of a tree that can be separated from the rest of the diagram by a single cut.

does not obey eq. (2.3), and we have therefore considered type-II approaches. In order to keep the present discussion at a non-technical level, we limit ourselves here to saying that for the sake of this work, and for future versions of MADGRAPH5_AMC@NLO, we have implemented a type-IIb solution. However, further details are provided in appendix A.

2.2 Matching to parton showers

The matching of matrix elements to parton showers in the presence of coloured intermediate resonances in s-channels presents some non-trivial features irrespective of the perturbative order at which it is carried out. In order to simplify the following discussion we shall always refer to the process we study in this paper; however, it should be clear that our considerations and procedure are valid in general. At the parton level, simulations for off-shell non-resonant single-top hadroproduction are based on processes of the type $xy \rightarrow Wbq(+z)$, rather than on their on-shell analogues $xy \rightarrow tq(+z)$. Therefore, there is no physical way (nor *formal* necessity) of flagging a specific subset of generated events as stemming from top-quark contributions. Nonetheless, despite the formal categorising of events as containing or not containing an intermediate top being unphysical, the description of higher-order contributions induced through parton showering might be very different in the two cases.

MC event generators typically handle the showering from a coloured resonance and from its decay products in a factorised fashion: emissions from the resonance are treated first and are in competition with all other sources of radiation, and emissions off the resonance decay products are added in a second, separate step. This choice is physically motivated by the NWA, which dictates a factorisation into production and decay subprocesses, as well as a suppression of the interference of radiation in production and in decay by $\Gamma_t/m_t \ll 1$. In the presence of a top-quark resonance, the showers from its decay products will usually be forced to preserve the reconstructed top invariant mass $m_t^{\rm rec}$ (to be precisely defined below). On the other hand, no such constraint is applied if the information on the intermediate top quark is absent. Such a disparity may lead to very different shower evolutions[2] even when starting from exactly the same final-state kinematics. For certain observables, especially those related to the invariant mass of the Wb-jet system, Wbq samples for which the top quark is not written in any of the events may thus produce results in visible disagreement with analogous on-shell $t(\rightarrow Wb)q$ samples, even in the narrow-width limit. The reconstructed top-quark mass is itself a prime example of this issue. This situation is disturbing, since it is ultimately due to *arbitrary* choices made in MC modelling. That is, despite being physically motivated, the decision of whether or not to write the resonance in the event record (which is based on the NWA that breaks down precisely in the off-shell region which one aims to investigate), and the constraint that the resonance mass is kept constant if written in the event record, are both choices that are non-parametric in nature. These can therefore easily offset the increase in precision attained by computing

---

[2]The verb "may" is emphasised here. In fact, the type of direct and indirect effects that could be seen in the final state crucially depend on the details of the specific MC implementation. We shall give explicit examples in section 3, for the cases of PYTHIA8 and HERWIG6.

higher-order corrections. At the same time, this implies that systematic studies of these aspects of MC modelling can sensibly be carried out also at the LO.

Pending thorough comparisons with data, at the theoretical level one can assume the on-shell-top limit of the showered results to be a sensible benchmark. Hence, the discussion above suggests that the explicit presence of the intermediate top in a Wbq sample is a desirable feature under certain conditions. The most straightforward example of the latter is that kinematic configurations for which m_t^{rec} is "sufficiently close" to the pole top mass m_t should include an intermediate top quark at the level of hard events to be given in input to the shower. Evidence for this feature comes from the fixed-order results, where it can be shown that near top-quark resonances, the dominant contributions to the cross section arise from Feynman diagrams involving intermediate top quarks [35–37]. It would appear consistent that the leading topologies at fixed-order should also be the dominant ones after parton-showering, and the presence of intermediate top quarks in Wbq samples would allow for this.

The strategy we have adopted in MADGRAPH5_AMC@NLO works essentially in the same way at the LO (where it was already the default [60]) and at the NLO. It is completely general, and is not restricted to the Wbj process we are considering in this paper. Moreover, it is already used, in a simplified format, for resonances that are not charged under QCD. The method relies on the adaptive multi-channel integration, in which integration channels are roughly in one-to-one correspondence with Born-level Feynman diagrams.[3] When considering a single integration channel, the corresponding diagram has a well-defined structure, possibly with intermediate s-channel contributions. We use this information to decide whether any of these intermediate resonances is written in the hard-event record. In particular, for each of such resonances:

a.) If the diagram that defines the integration channel does not feature the intermediate resonance in an s-channel configuration, then that resonance is not written in the hard-event file.

b.) If the diagram contains a resonance in an s-channel configuration, then we distinguish various cases depending on the FKS sector which is presently integrated, as follows.

b.1) If the diagram and the FKS sector are such that the grandmother of the real-emission radiation can be identified with that resonance (this is the situation depicted in the right panel of figure 1) the resonance is written on the hard-event record, and a type-IIb re-mapping is used, as outlined in section 2.1 and appendix A.

b.2) The procedure of item b.1) is always carried out in the relevant FKS sector, *except* in the two following cases: either the MC one matches to does not conserve the reconstructed resonance mass when off-decay emissions occur;[4] or a kinematic configuration is generated such that the re-mapping cannot be performed

---

[3]Even in the NLO mode of MADGRAPH5_AMC@NLO, the integration channels correspond to the underlying Born diagrams only — see section 6.3 of ref. [52], with $f = 1$.

[4]In this work this happens with PYTHIA8 in the global-recoil scheme..

(see appendix A). In these cases, no information on the resonance appears in the hard event.

b.3) For all of the other FKS configurations or at the LO, we use a dimensionless number, x_{cut}, to determine whether the resonance will be part of the hard-event record.[5] In detail, if and only if the given kinematic configuration satisfies the condition

$$\left| m_\beta^{\mathrm{rec}} - m_\beta \right| < x_{\mathrm{cut}} \Gamma_\beta \tag{2.10}$$

will the resonance be part of the hard-event record. The quantity m_β^{rec} denotes the reconstructed mass of the resonance β, and is *defined* as the invariant mass of the four-momentum sum of all the decay products of the resonance, as determined by the diagram used in the multi-channel integration (and the FKS sector in the case of real-emission-like events); x_{cut} is a free parameter.

What is done here is not motivated by considerations of numerical stability, as in the fixed-order NLO (fNLO henceforth [49]) computation (stability is merely a by-product in the present case), but rather by the fact that it is in keeping with the procedures adopted internally by the MCs. This implies that the construction of the MC counterterms relevant to the MC@NLO matching is modified in order to take the above information into account. In particular, the features described in items a.) and b.) are applied to the MC counterterms as well, in order to precisely mimic the kinematic constraints imposed by the PS at $\mathcal{O}(\alpha_s^{b+1})$. It should thus be clear that the only new ingredient w.r.t. the current implementation in MADGRAPH5_AMC@NLO is one relevant to emissions off the resonance decay products, which, being a phase-space re-mapping, can be trivially automated.

A couple of comments on the procedures adopted in MCs are in order here. Firstly, for emissions that do not involve s-channel resonances (left panel of figure 1, that corresponds to item b.3) above) MCs can easily, and do in the cases considered in MAD-GRAPH5_AMC@NLO, conserve m_β^{rec}, regardless of whether the resonance is written on the event record. Therefore, the dependence of physical observables on the parameter x_{cut} is not induced by the conservation (or the lack thereof) of the reconstructed resonance mass, but by the different behaviours of the showers driven by the presence of the resonance in the event record — we shall see explicit examples of this in section 3. Secondly, and as far as emissions off the resonance decay products are concerned (right panel of figure 1), in the case of HERWIG6, m_β^{rec} is conserved, whilst in PYTHIA8 it is not (owing to global recoil). In the MADGRAPH5_AMC@NLO matching to PYTHIA8, the global-recoil strategy is adopted in the latter, which allows one to simplify the MC counterterm definition in the former. In particular, the presence of resonances is ignored, since radiation from the decay products is generated identically to any other hard-process external partons, which means that the same evolution kernels, phase-space boundaries and kinematics are applied for similar evolution steps. Thus, all final-state particles compensate for the momentum shifts necessary to give non-null virtuality to the radiating parton. In the case of top decays, this

---

[5]In principle, the use of x_{cut} can be envisaged in item b.1) as well. We have refrained from doing so, for the reasons explained further below in the main text.

ultimately implies that the invariant mass of the Wb system (before an emission) and the invariant mass of the Wbg system (after an emission) are not identical. For this reason, as already mentioned in general in item b.) above, in the case of Pythia8 we do not apply a type-IIb phase-space re-mapping. We have further explicitly checked that, at the LO, differences between the global and local (which is m_t^{rec}-preserving) recoil schemes are negligible[6] for all differential distributions studied in the context of this paper (a sample of which will be presented in section 3).

We remark that one can envisage the possibility of introducing an x_{cut} dependence for emissions off the decay products as well (i.e. of using the condition of eq. (2.10) to decide whether or not to perform a re-mapping). We have presently refrained from doing so for a couple of reasons. Firstly, it is technically more complicated at the matrix-element level. Secondly, this effort would not really be justified in view of the fact that the Breit-Wigner function is steeply falling, and thus even for relatively small values of x_{cut} one is actually quite close to the asymptotic case $x_{\mathrm{cut}} \to \infty$. Because of this, in what follows Herwig6-based predictions have been obtained by setting $x_{\mathrm{cut}} = 35$ (our default, with 35 being our arbitrary choice of a very large value, consistently with the Breit-Wigner lineshape), and compared to those obtained with $x_{\mathrm{cut}} = 0$ (in which case, we disallow the type-IIb re-mapping in the phase space; this option will not be made available in the public version of MadGraph5_aMC@NLO). On the other hand, with Pythia8 these precautions are not necessary, and several values of x_{cut} will be considered.

While suitably writing the top quark in the hard events addresses the on-shell-limit issue, it poses another problem in the context of the MC@NLO matching. Despite the top quark not being an external particle in off-shell Wbq production, the factorised-shower structure described above allows MCs to radiate gluons both off the Wb system *and* off the top. The latter radiation may spoil the formal NLO accuracy of the computation. In fact, since gluon emission from an intermediate resonance is not IR-singular, in the context of the MC@NLO approach it is not associated with an MC counterterm, whence a potential double counting with the radiation of MC origin mentioned before.

Two solutions to this double-counting issue are possible: either a finite extra MC counterterm is added to the MC@NLO short-distance cross section in order to match at the NLO level the effects of the radiation off the top quark, or this type of radiation is directly disallowed in the PS. For simplicity, and without loss of formal accuracy, we have chosen the latter alternative,[7] but have nevertheless verified (by switching it on and off, which at least at the LO is fully consistent) that the impact of such top-quark radiation is negligible for all of the observables considered in this paper. The issue of double counting is specific to the NLO, and therefore no special measures regarding radiation from intermediate top quarks need to be taken at the LO; in our LO simulations, top quarks have been allowed to radiate.

---

[6]This is still not a proof that the same feature would hold at the NLO as well, but it is a strong indication that this is indeed the case. Note, furthermore, that in all the cases we have considered where Pythia8 and Herwig6 have significant shape differences, these are not due to the choice of recoil scheme in the former MC, but rather to the intrinsic different shower evolutions when these are (or not) "resonance-aware".

[7]We are grateful to Bryan Webber for providing us with a version of Herwig6 that disallows radiation off intermediate top quarks.

3 Results

3.1 Single-top hadroproduction: process definition and approximations

The starting point of the present work is the fNLO calculation for the t-channel single-top cross section in the five-flavour scheme presented in ref. [37], in which the reaction considered was[8]

$$p\,p \to W^+ \, J_b \, J_{\text{light}} + X. \tag{3.1}$$

As in typical single-top searches, at least two jets are present in the final state we study: a b-jet, J_b, defined as a jet containing the outgoing b-quark from the hard interaction (for this reason, we call this jet the *primary* b-jet), and an additional light jet, J_{light}, that does not necessarily contain bottom quarks. The assumption of a third-generation diagonal CKM matrix ($V_{tb} = 1$) is made in order to have a self-consistent definition of the t-channel process [37].[9] We remark that a consistent treatment of finite-width and non-resonant effects for top-quark production at NLO can be achieved through the use of the complex-mass scheme [38, 39]. This is a renormalisation scheme that introduces the top-width parameter Γ_t as part of a complex top-quark mass at the Lagrangian level. Examples of recent applications in NLO calculations with full off-shell effects are the NLO results for top-pair [41, 61–65] and t-channel single-top [37] production. In MadGraph5_aMC@NLO, the generation of the process of eq. (3.1) is obtained by issuing the following commands (see ref. [49] for details on the syntax, in particular table 14 at page 118 there):

```
./bin/mg5_aMC
MG5_aMC> import model loop_sm-no_b_mass
MG5_aMC> set complex_mass_scheme True
MG5_aMC> define p = p b b~; define j = p
MG5_aMC> generate p p > w+ b j $$ w+ w- z a QED=3 QCD=0 [QCD]
MG5_aMC> output; launch
```

As was discussed in ref. [37], a consistent definition of the process of eq. (3.1) in the five-flavour scheme requires a kinematic cut on the primary b-jet transverse momentum, which is not necessary when off-shell effects are neglected, i.e. when the top quark is taken to be stable. This constraint, which is relatively straightforward to impose when working at fixed order, becomes more complicated in the presence of parton showers, since it may become far from obvious which of the B-hadrons in the final state descends from the hard-interaction b-quark. In order to directly compare our present results to previous work at fNLO [37], and to ensure that the conclusions presented below at the hadron level are in as close analogy as possible with those of ref. [37], we have chosen to exploit MC truth.[10] This

---

[8]We emphasise that even if in ref. [37] and in this paper we simulate W^+ (i.e. top) production, the case of W^- (i.e. antitop) production is fully identical.

[9]The inclusion of the s-channel contribution would require a refinement to the definition of the b-jet in order make the process well-defined. Moreover, note that the requirement that the production be EW implies that no Born-level channel features a gluon in the final state, regardless of the value of V_{tb}.

[10]In both the HERWIG6 and PYTHIA8 showers, the mother (`JMOHEP`) and daughter (`JDAHEP`) arrays in the event record are used to perform this identification. In the HERWIG6 analysis we also make use of the information on the space-time vertices (`VHEP`) where particles are produced.

$p_T(J_b) > 25$ GeV	$p_T(J_{\text{light}}) > 25$ GeV
$|\eta(J_b)| < 4.5$	$|\eta(J_{\text{light}})| < 4.5$
140 GeV $< M(W^+, J_b) < 200$ GeV	
k_t jet algorithm [66, 67], with $R_{\text{jet}} = 0.5$	

Table 1. Setup for process definition and analysis.

enables the tagging of the primary B-hadron, identified as the B-hadron originating from the outgoing b-quark from the hard interaction. We tag the primary b-jet as the jet that contains the primary B-hadron. In addition to the p_T cut on the primary b-jet, we impose other cuts at the analysis level, summarised in table 1, which we adopt throughout our simulations. They are identical to those of ref. [37], and thus allow for a direct comparison with that paper. We limit ourselves here to reminding the reader that this setup has been chosen so as to avoid artificial enhancements of non-resonant contributions, so that a meaningful comparison with the on-shell single-top simulations can be made.

Given that observables sensitive to the leptonic decays of the W boson are also of interest in single-top analyses (e.g. the invariant mass of the lepton+b-jet system, $M(l^+, J_b)$, or the transverse mass of the reconstructed top quark, $M_T(l^+, \nu_l, J_b)$), we consider a leptonically decaying W^+. For events passed to the PS, these decays are carried out by the showers themselves, whereas at fixed order we simply decay the W^+ isotropically in its rest frame (which is also what the MCs do). We note that in this way production spin correlations for the leptons are not included. While these may be phenomenologically important, they are not relevant for the assessment of the off-shell and non-resonant effects we are presently interested in, and therefore do not warrant the more involved process definition that would be necessary when generating directly leptonic matrix elements.[11]

In view of the process definition and of the cuts in table 1, one expects its on-shell analogue to constitute a reasonable approximation. Indeed, as it has been shown both in single top [35–37] and in $t\bar{t}$ [41–43] production, the NWA does an excellent job in approximating the fully-off-shell results for many distributions. However, since it does fail to capture the dominant effects in regions of phase space that are sensitive to the top off-shellness and to non-resonant contributions, misuse of the NWA may therefore introduce errors that vastly exceed the naïve estimate of $\sim \mathcal{O}(\Gamma_t/m_t)$, which ultimately may have a bearing on experimental procedures such as top tagging and top-mass extractions.

The presence of potentially large effects of this kind will be studied in the following through a systematic comparison of the W^+bj results with their on-shell counterparts, which we generically denote by tj. In tj production the top is a stable external particle, hence its radiation in the shower is consistently matched at the level of the MC@NLO short-distance cross sections. Thus, in this case, showering from the top *must* be allowed in order to avoid double counting: this is the usual procedure [23, 25]. The inclusion

---

[11]Having said that, the generation of the full process `p p > e+ ve b j`, i.e. the process with spin-correlated W-boson decays, is possible with the current version of MADGRAPH5_AMC@NLO.

of NLO corrections to tj production, while highly desirable, is largely incomplete from the phenomenology viewpoint, since it does not improve the description of the top decays (which is left to the MC), and does not include any non-resonant contributions. This situation is addressed in part by the use of the procedure of ref. [29], automated in MAD-GRAPH5_AMC@NLO in the module MADSPIN [68], which allows one to include both production and decay spin correlations, and to give a rough description of off-shell effects through a simple Breit-Wigner smearing. For this reason, in the following we shall always use tj predictions in conjunction with MADSPIN (which we denote by tj+MS). Although an improvement w.r.t. the "bare" tj results, these still do not contain NLO corrections to top decays, and fully ignore the non-resonant contributions to the W^+bj final state.

In summary, by systematically comparing fNLO, tj+MS NLO+PS, and W^+bj NLO+PS results, as well as their LO counterparts, we shall be able to assess the impact of a variety of mechanisms, since the above simulations are characterised by an increasing degree of complexity, owing to the inclusion of parton showers, of NLO corrections to decays, and of off-shell and non-resonant contributions.

3.2 Differential distributions

In this section we present our predictions for several observables, obtained with the different computational schemes discussed in section 3.1. All of these have been derived by setting the input parameters that enter the hard matrix elements as shown in table 2. The width value labelled by "NLO" in table 2 is adopted in the context of the W^+bj NLO+PS and fNLO calculations, whereas that labelled by "LO" is used in all the other cases. Theory uncertainties are estimated by varying the renormalisation and factorisation scales independently in the range $[\mu_0/2, 2\mu_0]$. These variations are performed automatically by MADGRAPH5_AMC@NLO in the course of a single run, thanks to the re-weighting technique introduced in ref. [69].[12] We point out that, for certain observables, the LO scale dependence may be pathologically small, since the Born cross section does not contain any α_s factor. We have refrained from reporting the uncertainties associated with PDF errors, chiefly in view of the fact that they affect equally the W^+bj and tj production processes. We have run the two MCs by adopting the respective default parameters, except for the PDFs, which have been taken equal to those used in the short-distance computations. The simulation of the underlying events is turned off, and in order to simplify the analysis B hadrons are imposed to be stable.

In the following, to each observable we associate a figure that contains two main panels, one for HERWIG6 and one for PYTHIA8, each accompanied by three insets. The main panels display four curves: W^+bj results at NLO+PS and LO+PS with $x_{\text{cut}} = 35$ (solid and dashed blue, respectively), at fNLO (dashed green with full diamonds), and tj+MS results at NLO+PS (solid red with full circles). MADSPIN decays are characterised by a user-defined parameter, BWcut, that sets the allowed range (i.e. the distance, in width units, from the resonance pole mass) for the invariant mass of the system composed of the resonance decay products. We choose BWcut = 35 as our default, and indicate this explicitly

---

[12]This implies that the scale dependence of the top width is neglected.

$m_Z = 91.1876$ GeV	$m_W = 80.3980$ GeV
$\Gamma_Z = 2.4952$ GeV	$\Gamma_W = 0$ GeV
$G_F = 1.6639 \times 10^{-5}$ GeV^{-2}	$\alpha_e^{-1} = 132.3384$
$m_t = 173.2$ GeV	$m_b = 0$ GeV
$\Gamma_t^{\mathrm{LO}} = 1.5017$ GeV	$\Gamma_t^{\mathrm{NLO}}(\mu = m_t/2) = 1.3569$ GeV
Central scale: $\mu_0 = m_t/2$	PDFs: `MSTW2008NLO` [70]

Table 2. Input parameters for hard matrix elements.

by appending the value of `BWcut` to the label 'MS' in the plots (e.g. 'MS35' indicates MADSPIN results with `BWcut` = 35, and so on). We emphasise that the parameters x_{cut} and `BWcut` are technically different, even though they are both associated with a distance from the resonance pole mass. MADSPIN simulations feature a top quark in *all* of their Les-Houches events and therefore are independent of x_{cut} (more precisely, they are characterised by $x_{\mathrm{cut}} = \infty$) but depend on `BWcut`. Conversely, simulations of the full W^+bj process do not require MS decays, thus these events are strictly `BWcut`-independent, but do carry a dependence on x_{cut}. Still, x_{cut} and `BWcut` have a similar meaning from a physics viewpoint, because they parametrise, in different contexts, effects related to top-quark off-shellness. This is the reason why we have chosen their default values to be identical. Similarly, `BWcut` = 0.1 is the analogue[13] of $x_{\mathrm{cut}} = 0$.

The first (upper) inset in each figure contains ratios of the various perturbative approximations to the full W^+bj process: LO+PS/NLO+PS (solid blue), fLO/fNLO (dashed green), HERWIG6/PYTHIA8 at NLO+PS and at LO+PS (solid and dashed brown on the right, respectively), in addition to bands indicating the scale variations $\sigma^{(\mathrm{N})\mathrm{LO}}(\mu)/\sigma^{(\mathrm{N})\mathrm{LO}}(\mu_0)$ (HERWIG6 only, LO in yellow, NLO in grey on the left). The second (middle) inset contains the ratio, with respect to NLO+PS W^+bj with $x_{\mathrm{cut}} = 35$, of NLO+PS tj+MS with `BWcut` = 35 and with `BWcut` = 0.1 (solid red and dashed magenta, respectively) and of fNLO (dashed green). Finally, the third (lower) inset displays the ratio, with respect to NLO+PS W^+bj with $x_{\mathrm{cut}} = 35$, of NLO+PS W^+bj with $x_{\mathrm{cut}} = 0$, 1, and 5 (solid cyan, dashed red, and solid green, respectively, with the latter two values adopted only for PYTHIA8, as explained in section 2.2).

In order not to further complicate the discussion of the different effects that play a role in the results presented below, for each figure our analysis is structured as follows. After a brief overview of the observable examined and the important features of the fixed-order results (including the effects of NLO corrections, sensitivity to off-shellness, and non-resonant contributions), we address in turn:

a.) the effect of NLO corrections on the matched results for the full W^+bj process (first inset, solid blue curve);

---

[13]In MADSPIN one cannot set `BWcut` strictly equal to zero, and thus we have used 0.1 instead. Given the values of the top mass and width, this difference is fully irrelevant.

b.) the effect of parton showering with respect to the fixed-order results for the full W^+bj process (first and second insets);

c.) the differences between results for the full W^+bj process, showered with Herwig6 and Pythia8 (first inset, dashed and solid brown curves on the right-hand panels);

d.) the quality of the stable-top+MadSpin approximations to the full result (second inset, solid red and dashed magenta curves);

e.) the sensitivity of the results to the arbitrary x_{cut} parameter (third inset).

3.2.1 Transverse momentum of reconstructed top quark, $p_T(W^+, J_b)$

The first observable we examine is $p_T(W^+, J_b)$, the transverse momentum of the reconstructed top quark (defined as the system composed of the W^+ and the primary b-jet), shown in figure 2. This observable is inclusive in the invariant mass of the reconstructed top and is thus barely sensitive to off-shell effects [37]. Resonant/non-resonant interferences and pure non-resonant effects also do not play a major role. By comparing the fNLO results to MCFM [31] (t-channel single top in the NWA, with NLO corrections in both production and decay; not shown here) it can be deduced that the trend of the spectrum becoming harder at high $p_T(W^+, J_b)$ at fNLO w.r.t. fLO is a direct consequence of the corrections to production, but is however also enhanced by those to the decay.

a.) The inclusion of NLO corrections to the matched simulation mirrors the hardening of the spectrum observed when including NLO corrections at a fixed order.

b.) The dashed green curve in the second inset indicates that PS effects are on the whole not large (below 10% in all bins except the first bin for Pythia8), and do not significantly alter the shape of the fixed-order results.

c.) The agreement between Herwig6 and Pythia8 improves at NLO (the solid brown curve on the first right-hand inset is systematically closer to unity than the dashed brown curve). However, it should be pointed out that the agreement is already good at LO (especially shape-wise).

d.) The second inset reveals that there is a general trend of the tj+MS spectra becoming softer compared to those of the NLO+PS W^+bj results. This effect follows from the same reasoning as the softer behaviour of the fLO or the LO+PS spectra w.r.t. their NLO counterparts, but is of much smaller size since the MadSpin results do include radiative corrections to the production subprocess, while they lack those to the top decay. Overall, the results for NLO+PS tj+MS are in agreement with the full NLO+PS W^+bj ones to better than 10% for both showers, indicating that not only corrections to the decay but also non-resonant contributions are small in this case. Moreover, the invariance of the MadSpin results under variation of the `BWcut` parameter confirms that this distribution is relatively insensitive to off-shell effects.
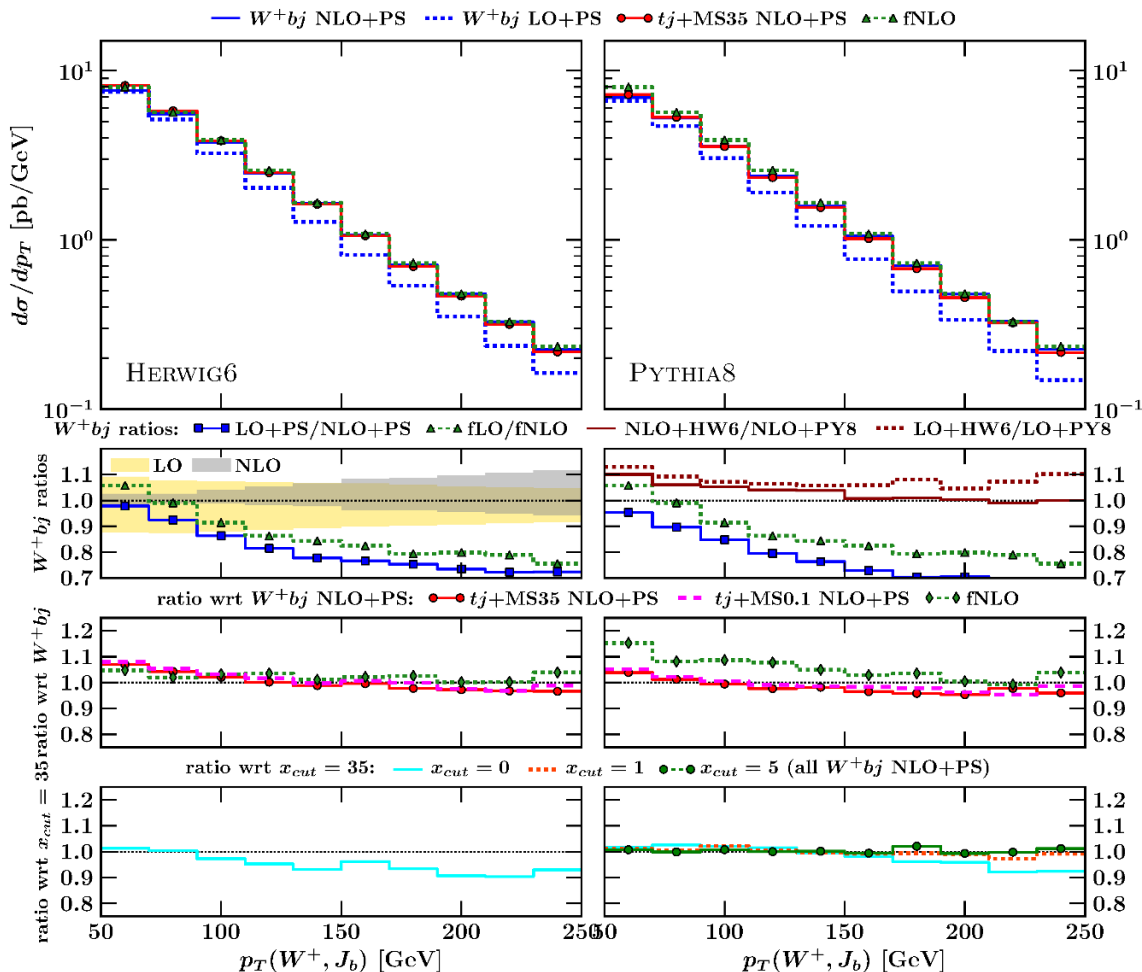
Figure 2. Transverse momentum of reconstructed top, $p_T(W^+, J_b)$.

e.) The third inset reveals that $p_T(W^+, J_b)$ is largely stable against the choice of x_{cut}, with only $x_{\text{cut}} = 0$ displaying any visible effects. The latter are however smaller than (PYTHIA8) or comparable to (HERWIG6) the NLO scale uncertainty illustrated by the band in the upper left inset.

3.2.2 Transverse momentum of primary b-jet, $p_T(J_b)$

Figure 3 shows the transverse momentum of the primary b-jet, $p_T(J_b)$. This observable is less inclusive than $p_T(W^+, J_b)$ over the top decay products, and therefore NLO corrections to the decay are expected to play a more important role. This is indeed the case since the non-trivial shape at low p_T of the differential K-factor at fixed order is driven by the NLO corrections to the top decay (this has again been cross-checked with MCFM). These corrections also result in a harder $p_T(J_b)$-tail at NLO w.r.t. LO. The feature at small p_T in the fLO/fNLO ratio can be attributed to the kinematical fact that real radiation off the b-quark carries energy away from the b-jet, thus softening the NLO spectrum; such a leakage occurs less often when moving towards large p_T's, where the jets tend to be more collimated.
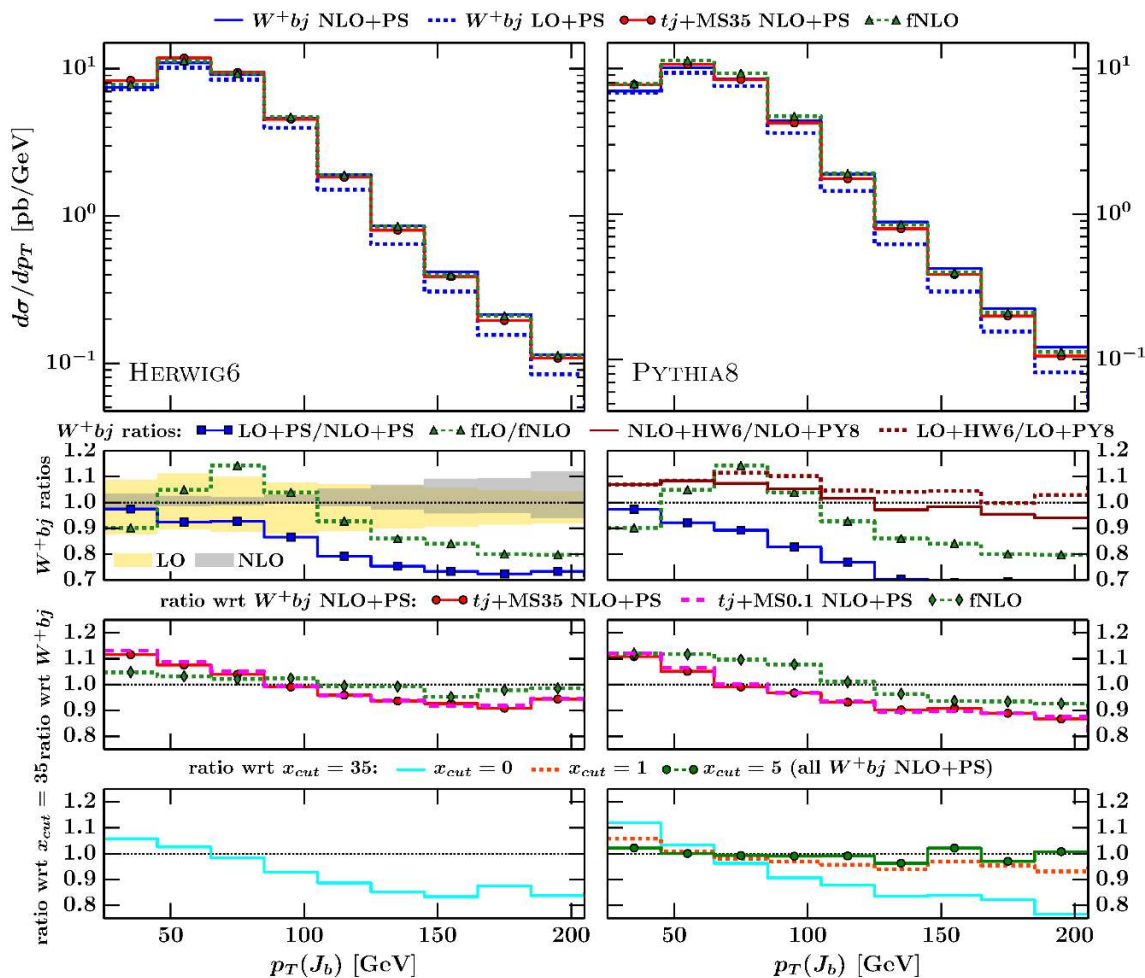
Figure 3. Transverse momentum of primary b-jet, $p_T(J_b)$.

a.) The differential K-factors for the showered results at large values of $p_T(J_b)$ display the same features as the fixed-order results (NLO+PS distributions are harder than LO+PS ones). However, the kinematic suppression in fLO/fNLO at low $p_T(J_b)$, driven by the fLO shape, does not carry over to the showered case. This is due to the fact that the shower, already at the LO, accounts for multiple emissions from the final-state b quark, hence the radiation leakage outside the b-jet, induced by real corrections in the fixed-order case, has a much milder impact at the showered level.

b.) The dashed green curve in the second inset indicates that the shower effects for HER-WIG6 at NLO are small, i.e. that NLO+PS is very close to fNLO, with a distribution only marginally harder ($\pm 5\%$ at low and high $p_T(J_b)$, respectively). With effects of around $\pm 10\%$, PYTHIA8 departs more from the fNLO result.

c.) From the brown dashed and solid curves in the upper right inset, we conclude that there are only mild shape differences between the HERWIG6 and PYTHIA8 predictions; PYTHIA8 tends to be slightly harder than HERWIG6. The ratio of the two MC predictions displays a more regular behaviour (i.e. in a larger p_T range) at the NLO

than at the LO. This is most likely due to the fact that the impact of the matrix-element normalisation constraint is more important in the former than in the latter case. Such a pattern is similar to that observed in the case of $p_T(W^+, J_b)$ but is of slightly bigger size here, which is consistent with the fact that the present observable is more dependent on MC modelling than the transverse momentum of the pseudo top.

d.) The trend of the NLO+PS tj+MS curves (solid red, second inset) closely follows that of the LO+PS W^+bj predictions, namely they are softer than the NLO+PS W^+bj benchmarks. The effect is similar to that observed in $p_T(W^+, J_b)$ but is somewhat more pronounced here. Given that at fNLO in the NWA it is the corrections to the decay that induce the dominant features of the fLO/fNLO ratio, and that it is precisely these corrections that are missing in the MADSPIN results, this is a strong indication that corrections to the decay subprocess are important for this observable. The independence of the MADSPIN result on the BWcut parameter indicates that off-shell effects are essentially irrelevant for this observable — a feature that can also be seen at fixed order.

e.) As for the case of $p_T(W^+, J_b)$, the present observable is relatively insensitive to the value of x_{cut}. We only observe a marked effect for $x_{\text{cut}} = 0$, with differences to the $x_{\text{cut}} = 35$ result of up to 20% in the hard tails, for both showers.

3.2.3 Invariant mass of reconstructed top quark, $M(W^+, J_b)$

The reconstructed top quark mass, $M(W^+, J_b)$, displayed in figure 4, is an important observable used to tag top quarks and to help separate the single-top signal from its backgrounds. It may also be used in various ways to extract the top mass from data. At fixed order, the real-radiation corrections to both production and decay are important and are the dominant contributions to the shape of the fLO/fNLO ratio. The region above the peak is sensitive to radiation from the production subprocess, whereas the region below the peak is sensitive to radiation from the top decay products. Additionally, treating the top quark as off-shell is vital to sensibly describe this distribution at fixed order, with the predictions using the NWA failing to capture most of its features; see ref. [37] for more details.

a.) The effect of the NLO corrections on the LO+PS curve is to skew the distribution towards the right. The agreement in shape between LO+PS and NLO+PS in the low-mass region, i.e. the region sensitive to radiation from the final-state b-quark, is satisfactory for both showers (and slightly better for HERWIG6). This is an indication that for this observable, and in this phase-space region, hard radiation originating from the top-quark decay products is well approximated by the parton showers. The harder spectra at NLO+PS, particularly visible from the large-mass slope of the HERWIG6 result, stem from hard radiation in the production subprocess being clustered into J_b by the jet algorithm. The PYTHIA8 high-mass tail does not show as strong a trend as HERWIG6, likely pointing to more (or harder) production radiation in the LO results compared to the HERWIG6 shower. The fact that this behaviour is mostly driven by the LO predictions can be inferred from the two brown histograms in the upper right-hand inset — see item 3 below.
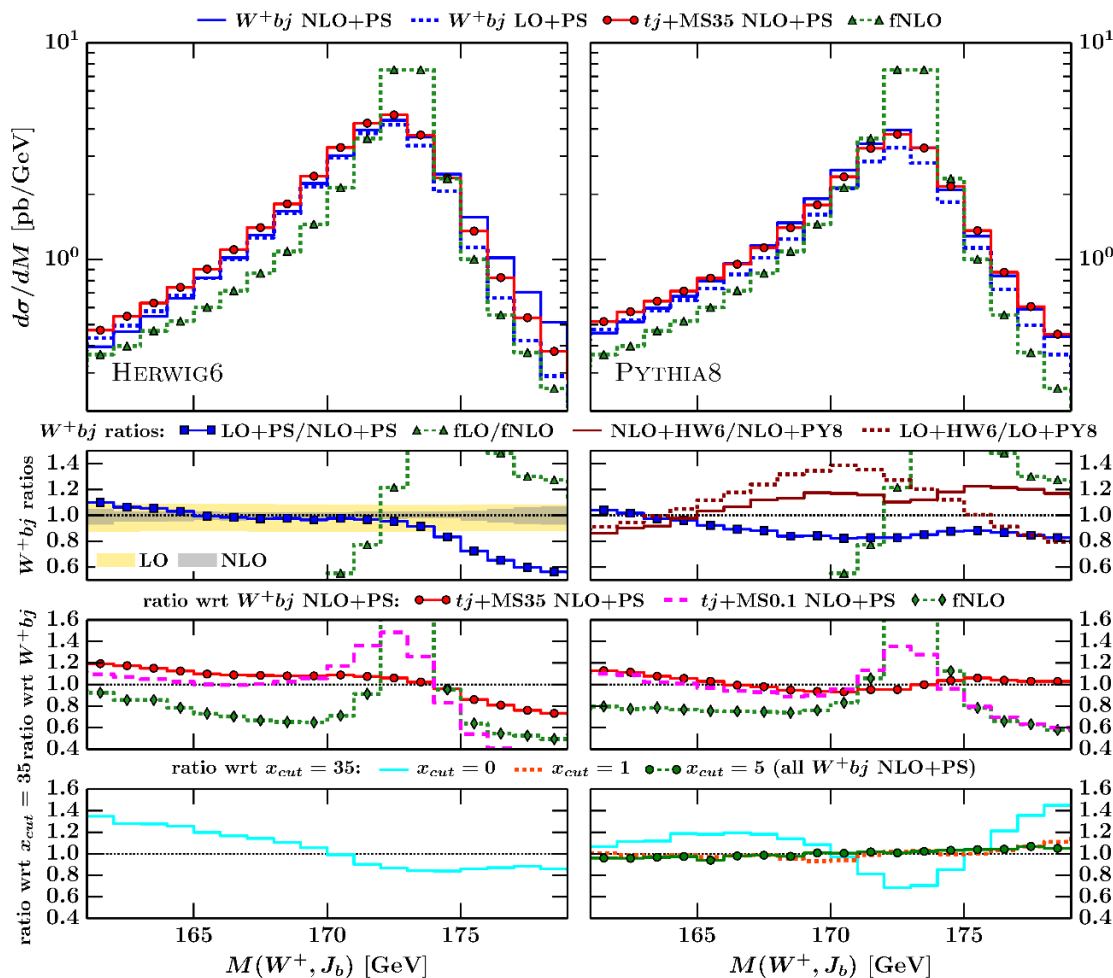
Figure 4. Invariant mass of reconstructed top, $M(W^+, J_b)$.

b.) The effect of parton showering with respect to fixed-order results is very significant over the full range considered, and exceeds 50% in the bins near the peak. Radiation by both showers smears and flattens the sharply-peaked fixed-order distribution. This smearing results from the combined effect of ISR and FSR enhancing the high-mass tail when clustered into the b-jet, and of b-quark FSR enhancing the low-mass tail when leaking out of the b-jet.

c.) The dashed and solid brown curves in the first right-hand inset indicate that, both at LO and NLO, the PYTHIA8 distributions are flatter overall than the corresponding HERWIG6 ones, with effects as large as 20% and 40% at NLO and LO, respectively. Despite the remaining visible differences, there is a substantial improvement in the consistency of the two showers at NLO, compatible with the increased formal accuracy of the simulation. Differences between the two showers are to some extent expected — the smearing cannot be attributed to one single factor, but rather is a combination of various sources that vary between the showers: different $\alpha_s(m_Z)$ or Λ_{QCD} choices, different showering models (interleaved ISR/FSR in PYTHIA8 and sequential ISR/FSR in HERWIG6) and different hadronisation models.

d.) The results for tj+MS are, for large values of BWcut, in good agreement (20% or better in the case BWcut = 35) with the NLO+PS W^+bj distributions. This is particularly true for PYTHIA8, especially above the peak, while in the case of HERWIG6 the tj+MS result displays a softer behaviour over the full mass range considered. As for the observables considered previously, for both showers the tj+MS/W^+bj ratio has a similar pattern, though milder (i.e. it is closer to one), as that of the W^+bj LO+PS/NLO+PS ratio. The large discrepancies between the BWcut = 35 and BWcut = 0.1 results, which are significant close to the peak (and, to a lesser extent, above it), indicate the importance of including off-shell effects for a good description of this observable in that region. On the other hand, all BWcut choices appear to be in good mutual agreement below the peak. This is likely due to off-shell effects being subdominant in this region w.r.t. corrections to the top decay products.

e.) $M(W^+, J_b)$ exhibits a sensitivity to $x_{\rm cut}$ qualitatively similar to that seen for $p_T(J_b)$ and $p_T(W^+, J_b)$, namely there is a very small dependence for $x_{\rm cut} \geq 1$, while the extreme choice $x_{\rm cut} = 0$ gives some visible shape distortions.[14] For both MCs the $x_{\rm cut} = 0$ results are flatter, more markedly so with PYTHIA8, which has also a mild tendency to skew the distribution rightwards, while in the case of HERWIG6 the skewing is rather leftwards. This shows that, when the MCs have no information about the intermediate resonance, large model-dependent effects can be introduced in the resonance structure. In the region of $M(W^+, J_b)$ above the peak, PYTHIA8 appears to be significantly more sensitive than HERWIG6 to the choice of $x_{\rm cut} = 0$. This is related to the different construction principle underlying the showering models. While HERWIG6 first generates initial-state radiation, and follows up by generating final-state emissions, PYTHIA8 constructs both showers in a combined, interleaved sequence. Thus, initial- and final-state radiation are in direct competition in PYTHIA8. This competition is drastically different for $x_{\rm cut} = 0$ and $x_{\rm cut} = 35$. In general, the PS can emit from the initial-state partons, the light final-state partons, and from the top-quark decay products. In the $x_{\rm cut} = 0$ case, all of these possibilities compete with each other for phase space. In the $x_{\rm cut} = 35$ case, the evolution is split into showering the production process, and showering the decay products. Thus, while all partons associated with the production process compete with each other, the radiation off the decay products is not encumbered by any competition.[15] These different mechanisms — due to the different evolution prescriptions in the $x_{\rm cut} = 0$ and finite $x_{\rm cut}$ cases — lead to the $x_{\rm cut}$ dependence seen in the PYTHIA8 results.

It is beyond the scope of this work to decide which showering model (interleaved versus independent) is preferable. We have instead chosen to document the features

---

[14]This statement depends on the pseudo-top mass range considered. If plotted in a range wider than that of figure 4, the $x_{\rm cut} = 1$ and $x_{\rm cut} = 5$ results (the former to a much larger extent than the latter, as expected) would also exhibit increasingly large differences w.r.t. the $x_{\rm cut} = 35$ one.

[15]Note that the absence of competition does not mean the absence of constraints, since overall phase-space boundaries and momentum conservation have to be respected. For example, if no radiation off other legs were present, then the constraints for radiation off the b quark would be independent of $x_{\rm cut}$, in the global recoil scheme.

related to this choice for the process under consideration, and regard the x_{cut} dependence as a way of parametrising this modelling uncertainty. The fact remains, that by never writing the top on the hard-event record, one becomes more sensitive to the different underlying shower mechanisms.

3.2.4   Mass of primary b-jet, $M(J_b)$

Next, we examine the invariant mass of the primary b-jet, $M(J_b)$, displayed in figure 5. Due to the analysis setup we have adopted (specifically the requirement of both a b-jet and a light jet in the final state), at fLO $M(J_b)$ only receives contributions in the first bin, $M(J_b) = m_b = 0$. At fNLO, the region $M(J_b) > 0$ is filled by events where real radiation is clustered together with the b-quark to form the b-jet. Since only real radiation contributes non-trivially in this region, the fNLO prediction diverges as $M(J_b) \to 0$. Shower effects are dramatic: the threshold is shifted from zero to the mass of the lowest-lying B hadron, and the low-mass divergence present at fixed order is offset by the usual Sudakov damping. Consequently, discrepancies in this case are expected to be significant, both in the comparison between NLO+PS and fNLO results, and between different MCs. We point out that the characteristics of the present observable outlined above render it analogous to any quantity which has only kinematically-trivial contributions at fLO, meaning that it displays maximal sensitivity to real radiation and to the shower. In these cases, a by-product of matching to showers is also that of featuring an NLO-type scale uncertainty in the region which receives solely non-hard real-emission contributions. This analogy only holds to a certain extent here since, for the b-jet mass, hard (as opposed to soft) real radiation cannot be associated with certainty to a specific region of the phase space. For example, a hard emission from the initial state could be nearly collinear to the final-state b-quark, yielding a small b-jet mass. However, one expects the impact of these configurations to be subdominant.

Jet masses will, in general, aside from an increased sensitivity to perturbative effects (including NLO-matching systematics), also show a relatively strong dependence on non-perturbative and soft-physics modelling; this is particularly true at small masses. Therefore, any conclusion based on varying only "perturbative parameters" is potentially incomplete.

a.) Including NLO corrections when matching to parton showers leads to a harder $M(J_b)$ distribution in the case of HERWIG6, while induces only a constant shift for PYTHIA8. In both cases the effects are relatively mild (up to 20% for HERWIG6, and 10% for PYTHIA8), which is remarkable if compared with the situation at fixed order.

b.) The effects of parton showering for $M(J_b)$ lead to completely different distributions with respect to fixed-order results; the latter are indeed not particularly sensible for an observable of this type. As discussed before, this stems from two main reasons. Firstly, at fixed order the bins for $M(J_b) > 0$ only receive contributions from real corrections. Secondly, b-jets are reconstructed at the hadron level, and hence their mass threshold is close to the physical mass of B hadrons. We remark, however, that even if b-jets were reconstructed at the parton level in (N)LO+PS simulations,
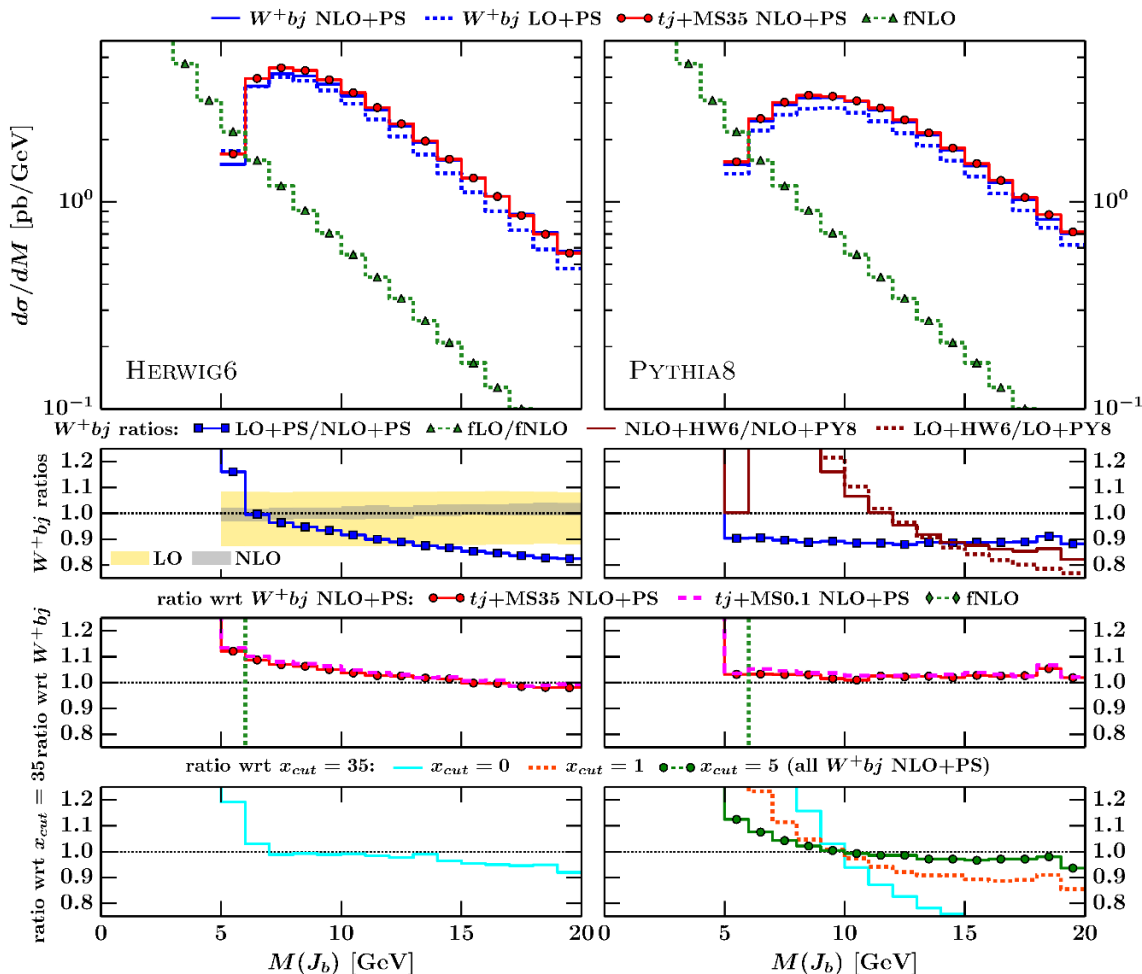
Figure 5. Mass of primary b-jet, $M(J_b)$.

one would obtain a very similar threshold, owing to the fact that the MCs need to turn b quarks into massive objects with $m_b^{\mathrm{MC}} \sim 5\,\mathrm{GeV}$, in order to give a realistic description of b-physics phenomena.

c.) The comparison between PYTHIA8 and HERWIG6 reveals sizable differences, compatible with the fact that this observable receives large contributions both from higher perturbative orders and from the underlying showers. Nevertheless, given the behaviour of the fixed-order results, the (N)LO+PS predictions appear to be reasonably close to each other and, in addition, by including the information on the NLO matrix elements the differences seen at LO+PS are reduced. In particular, it is reassuring that the agreement between HERWIG6 and PYTHIA8 improves to about 15% in the medium- and high-mass regions. There is also an improvement at low jet masses (not visible in figure 5), which however should not be over-interpreted, since non-perturbative effects are expected to be substantial in this region.

d.) The solid-red and dashed-magenta lines in the second inset indicate that the MAD-SPIN results roughly follow similar shape patterns as those of LO+PS W^+bj, namely

that they are softer than NLO+PS W^+bj for Herwig6, and flat for Pythia8. However, in absolute value they are in much better agreement than the LO+PS results with the NLO+PS W^+bj predictions. The MadSpin results show no dependence on the BWcut parameter, indicating that off-shell effects do not have an impact on the shape of $M(J_b)$.

e.) The third inset shows that Herwig6 and Pythia8 have a vastly different dependence on x_{cut}. The results showered with Herwig6 are mostly independent of x_{cut} (except in the low-mass region), while those showered with Pythia8 are highly sensitive to this parameter over the whole range considered. As for the case of $M(W^+, J_b)$, this behaviour can be attributed to the different showering models. The Pythia8 sensitivity of the b-jet kinematics on x_{cut} does indeed largely drive the x_{cut} variation of the reconstructed-top mass that we have observed previously.[16] Radiation from the b-quark is the primary source of mass increase in the region of moderate b-jet masses, i.e. $M(J_b) \gtrsim 10\,\text{GeV}$, with other phenomena playing only a subdominant role there (contributions from splash-in radiation off other legs become more important at larger masses, which we do not show in figure 5). For a vanishing x_{cut} value, as discussed in item 5 of section 3.2.3, this radiation is always in direct competition with radiation off all other initial and final state partons, forming a single evolution chain. Conversely, for non-null values of x_{cut} the radiation off the b starts without competition. Thus, it turns out that in this case non-competing radiation off the b quark fills the b-jet more substantially, and leads to a heavier jet. Such an x_{cut} dependence diminishes at larger $M(J_b)$, owing to off-b radiation no longer being dominant. The behaviour at low $M(J_b) \lesssim 10\,\text{GeV}$ is also due to the choice of cuts on the b-jet. Lowering the $p_T(J_b)$-cut in particular leads to a less marked shape difference between the low- and high-x_{cut} results. Crucially, we have checked (with LO simulations) that the same x_{cut}-variation pattern in Pythia8 is found when using the local recoil. Hence, the striking feature seen in the comparison of the Pythia8 and Herwig6 results is not due to the recoil scheme we have adopted.

We conclude this section by re-iterating the message that figure 5 must be seen in its entirety: differences between generators are as important as perturbative uncertainties, and can suggest strategies to improve the description of $M(J_b)$. Furthermore, we point out that this observable is also quite sensitive to effects controlled by tuning and underlying-event modelling, which we have not studied here.
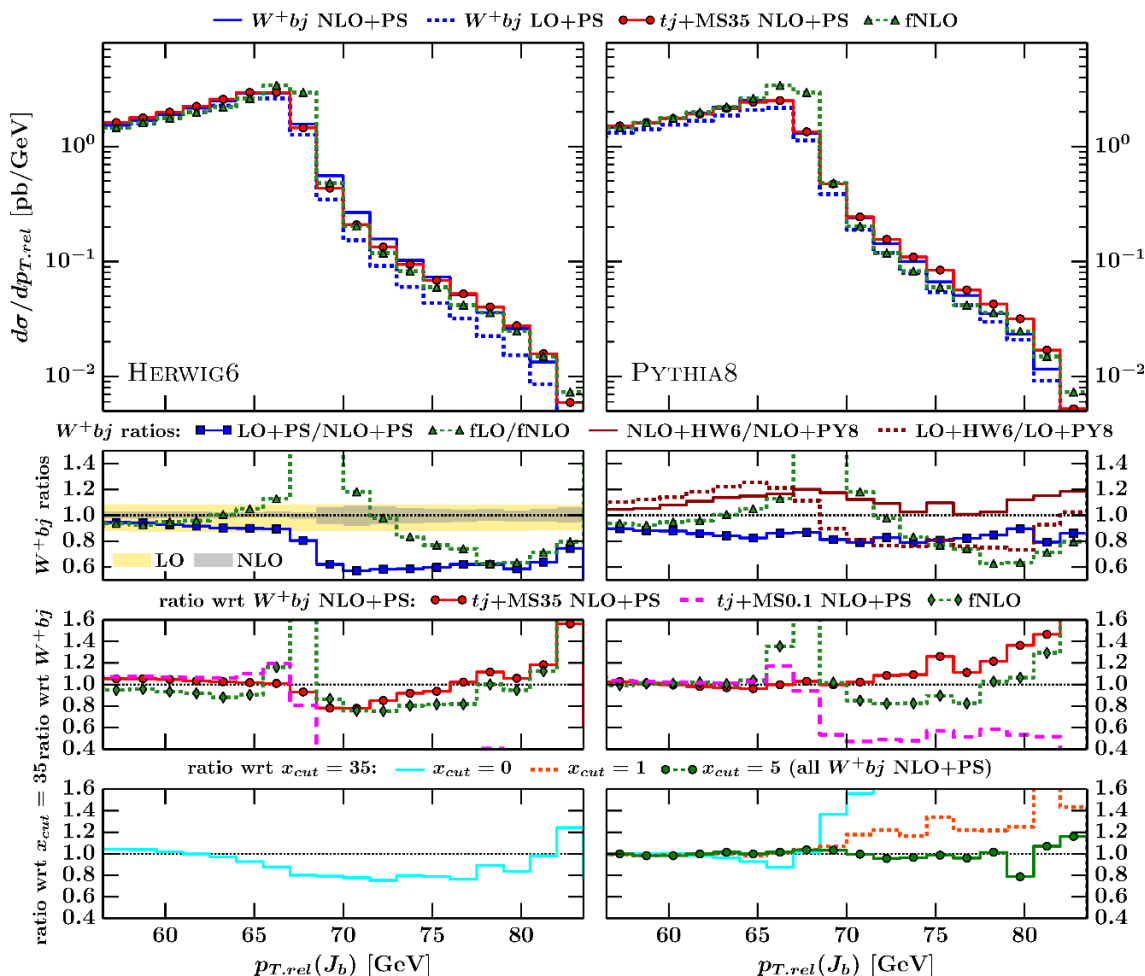
3.2.5   Relative transverse momentum of primary b-jet, $p_{T,rel}(J_b)$

We now turn our attention to the transverse momentum of the primary b-jet in the reconstructed top quark rest frame, relative to the direction of flight of the reconstructed top quark. We denote this quantity by $p_{T,rel}(J_b)$, and display it in figure 6. This observable

---

[16]We remark that the x_{cut} dependence of $M(J_b)$ is subdominant as far as the behaviour of the reconstructed top mass is concerned. In the case of $M(W^+, J_b)$, the x_{cut} dependence is chiefly driven by changes in the direction of flight of the b-jet, which renders the $M(J_b) - M(W^+, J_b)$ correlation a rather non-trivial function of x_{cut} and of the mass ranges considered.

Figure 6. Transverse momentum of primary b-jet, $p_T(J_b)$ in top quark rest frame, relative to the direction of flight of the reconstructed top quark.

is challenging to simulate accurately because its shape is — already at fixed order — the result of a balance between different kinematical effects. The sharp edge present in this distribution corresponds to the value $p_{T,rel}(J_b) = (m_t^2 - m_W^2)/2m_t$. In the NWA at fLO, transverse momenta larger than this threshold are kinematically forbidden; the tail beyond the edge starts appearing at fNLO, due to real corrections to the production subprocess. NLO corrections to the decay become important near the peak of the distribution, whilst at the peak and above it becomes crucial to treat the top quark as off-shell [37]. The shoulder of the distribution and the region above the peak are shaped by an interplay of contributions from real emissions that originate from the production subprocess, as well as resonant/non-resonant interference effects and pure non-resonant effects — the latter increasing in importance the further one goes into this region of phase space. The sensitivity of the shoulder and the tail of this distribution to m_t make it potentially a good observable for m_t-extraction, provided that the theoretical systematics are under control. Additionally, observables such as this one are well-suited to disentangling top signals from

QCD backgrounds. Therefore, it is imperative that MC predictions are fully understood, and faithfully describe any significant effects over the full range of p_T.

a.) Overall, it is apparent that the fixed-order K-factor, as in the case of $M(W^+, J_b)$, is smoothed out by the showers. In the region of the shoulder and below the peak, LO+PS and NLO+PS predictions are similar in shape for both showers. However, at the kinematic threshold and beyond, the NLO corrections result in a "step up" in HERWIG6 whilst in PYTHIA8 they do not induce such a change in shape. This is an indication of how copiously the PYTHIA8 shower populates this region with radiation already at LO.

b.) The effects of parton showering are mild in the low-$p_{T,rel}(J_b)$ region (especially for PYTHIA8), while they are very large at the sharp edge and also visible in the high-$p_{T,rel}(J_b)$ tail. The sharp edge at fixed order is made less steep through the combination of two effects. Firstly, near the edge (i.e. close to the fixed-order kinematical threshold) multiple FSR emissions off the b-quark leaking out of the b-jet lead to the lowering of the peak. Secondly, emissions from the production process captured inside J_b enhance the region beyond the sharp edge. We note that the high-$p_{T,rel}(J_b)$ region is predominantly LO-accurate in the context of the simulations performed in this paper,[17] hence the results are expected to have a larger sensitivity to the various approximations here than elsewhere. This is reflected in the shape of the scale-uncertainty band in the top-left inset.

c.) Considering the balance of different effects resulting in the shape at fixed order, the relative agreement between PYTHIA8 and HERWIG6 for this observable is encouraging. There is a clear improvement in the agreement when passing from LO+PS to NLO+PS, even in the high-tail region, where the cross section is reduced by 2–3 orders of magnitude with respect to the peak. The pattern of the HERWIG6 over PYTHIA8 ratio at the LO+PS level can be understood as due to the larger amount of radiation (from production) in PYTHIA8, which enhances the region above threshold, and thus, by unitarity, decreases the cross section below threshold. At NLO+PS this feature is very much reduced, with discrepancies smaller than 15% in most bins.

d.) For values of $p_{T,rel}(J_b)$ below the sharp edge, all MADSPIN results do a very good job in approximating the shape of the full result in both showers. However, beyond threshold, the differences between the two MADSPIN `BWcut` values, as well as the differences of these w.r.t. the full result, begin to grow significantly, reaching 50% or more at the edge of the range considered. By moving deeper into this region of phase space, as also pointed out in ref. [37], the result becomes increasingly sensitive to off-shell and non-resonant effects. Non-resonant contributions are missing in the MADSPIN results and therefore the differences between these and the complete NLO+PS W^+bj result can be expected. This comparison indicates that for this observable and in these regions of phase space the full NLO+PS W^+bj computation is a prerequisite for a reliable description.

---

[17]This is strictly true in the NWA, while off-shell effects partially fill the region beyond threshold already at fLO in the full W^+bj computation.

e.) There is a striking difference in the dependence of the HERWIG6 and PYTHIA8 results on the $x_{\rm cut}$ parameter. This is particularly pronounced beyond the edge in the spectrum, i.e. in the region where both real radiation and non-resonant effects are very important. The HERWIG6 distribution displays at most a 20% dependence on $x_{\rm cut}$. On the other hand, beyond the sharp edge the results showered with PYTHIA8 become very sensitive to $x_{\rm cut}$, a feature that stems from the same reasons as those already described in detail in item 5 of sections 3.2.3 and 3.2.4.

3.2.6   Invariant mass of lepton+b-jet system, $M(l^+, J_b)$

The relative transverse momentum discussed in section 3.2.5 can be seen as a member of a class of observables characterised by the presence of sharp edges due to thresholds in the NWA. Other examples are the invariant mass of the b-jet-lepton pair, $M(l^+, J_b)$, and the transverse mass of the system composed of the b-jet, the charged lepton, and the neutrino.[18]

These observables may have fairly different properties from the experimental viewpoint (in particular as far as the reconstruction of the candidate top pseudo-particle is concerned), the discussion of which is beyond the scope of the present work. On the other hand, because of the kinematic features they have in common, they display similar patterns in terms of the various theoretical approximations that can be used to predict them.

To exemplify this fact, in figure 7 we show the results for $M(l^+, J_b)$ (we remind the reader that spin correlations have been neglected in the leptonic decay of the W boson). This observable is often used as a discriminating variable to help disentangle top-quark signal events from backgrounds, and interestingly it has been employed to extract the top mass in t-channel-enhanced events [14]. As can be seen from the plots of figure 7, the conclusions of section 3.2.5 also apply, largely unchanged, to the present case.

Given that the different predictions have been studied in detail and are now available, it would be interesting to exploit these to quantify the systematic error on the extraction of m_t via $M(l^+, J_b)$ that is introduced through the use of generators that do not include full off-shell effects and NLO top-decay corrections.

4   Conclusions and outlook

In this paper we have studied t-channel single-top hadroproduction, where full off-shell and non-resonant effects are computed at the matrix-element level with NLO accuracy in QCD, and matching to parton showers is included. We have done so in the context of the automated MADGRAPH5_AMC@NLO framework, where we have implemented our solutions in a process-independent way. This constitutes the first example, in the MC@NLO approach, of the matching of an NLO calculation to a parton shower that features an improved treatment of intermediate coloured resonances.

We have considered two Monte Carlos, PYTHIA8 and HERWIG6, as representatives of different behaviours with regard to several characteristics, most notably shower evolution

---

[18]Strictly speaking, the pseudo-top mass itself also belongs to this category, but being extremely peculiar it constitutes a case on its own.
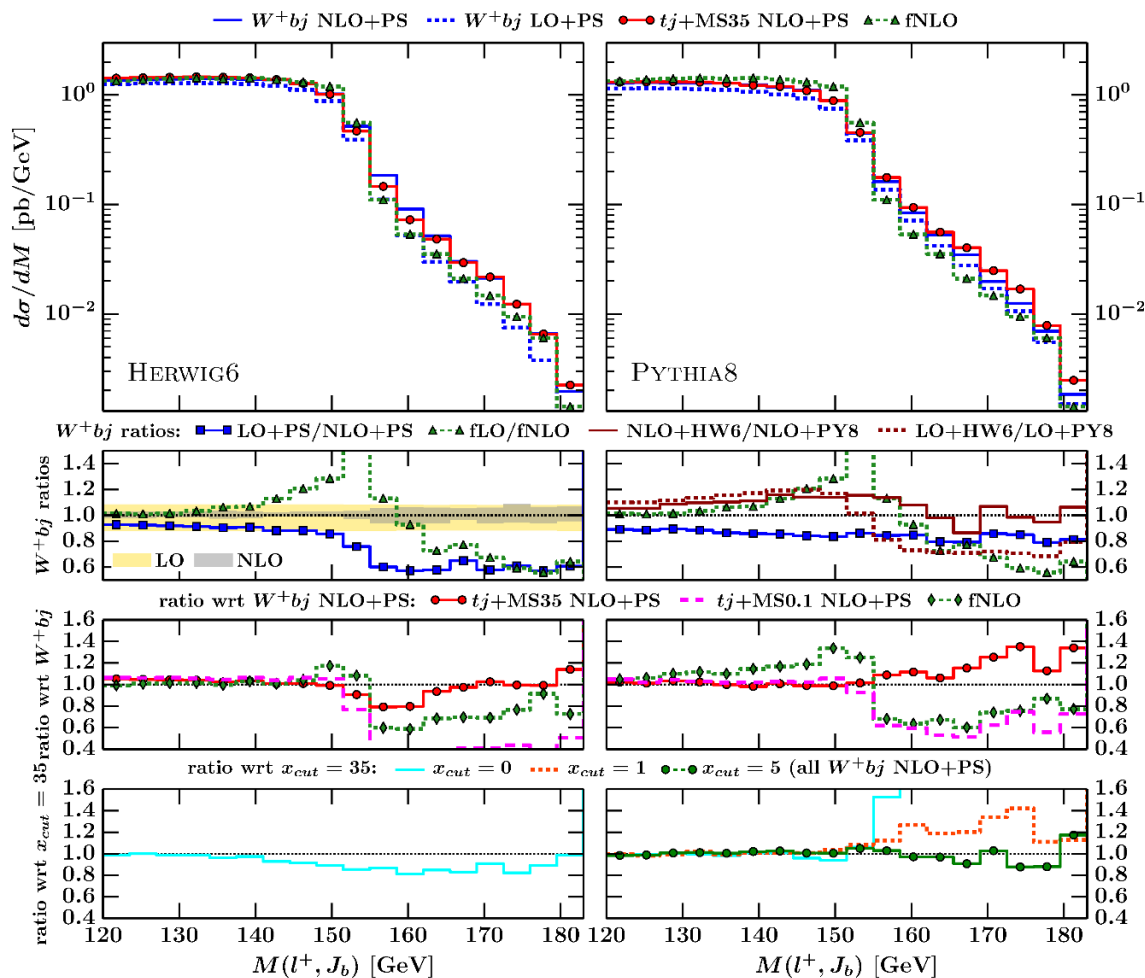
Figure 7. Invariant mass of lepton+b-jet system, $M(l^+, J_b)$.

and handling of resonances. This has allowed us to deal in detail with a few resonance-specific aspects of the matching. Among these were the definition of the MC counterterms necessary in the MC@NLO formalism, the treatment of resolved MC emissions off intermediate top quarks, and the writing of information on these tops in Les-Houches event files. The latter item, to a large extent, pertains to MC modelling, and it is thus important to keep in mind that the writing of an intermediate top in the hard-event file can significantly affect how the events look after parton showering. Although we have argued that including such information is certainly physically motivated, and is consistent with results obtained in the $\Gamma_t \to 0$ limit, we have studied its consequences by parametrising it by means of an arbitrary dimensionless quantity x_{cut}. It will be interesting to compare theoretical predictions, and their dependence on x_{cut}, with actual data.

We have obtained results based on a generic final-state analysis, chosen to be as similar as possible to that of the fixed-order calculation presented in ref. [37], in order to allow for a direct comparison to the latter paper. Overall, it is observed that for this typical analysis the differential K-factors at the hadron level can be large and non-constant in

shape. However, as expected, the scale dependence of the results generally decreases when going to NLO+PS accuracy. Our comparison to the fNLO predictions illustrates that effects of parton showering and hadronisation can be large (>10-15%). We also find that the agreement between the predictions of the two showers improves at NLO, though the differences themselves are found to be sizeable for some observables (in particular for the invariant mass of the primary b-jet).

An important consequence of the availability of predictions at NLO+PS accuracy, with full off-shell effects, is that existing approximations can be scrutinised and validated. We have made a detailed comparison to the results of stable single-top production at NLO+PS accuracy, where the spin-correlated decay of the top quark and the leading off-shell effects are included by using MADSPIN. On the whole, it is observed that the MADSPIN results describe the full results remarkably well, which is certainly encouraging in view of the fact that the predictions of the former type presently constitute the benchmark for simulations that involve coloured resonances at LHC experiments. However, we have observed some notable differences between stable-top and full results in some of the distributions we have studied, with an observable-dependent pattern. We have attributed these to NLO effects in the top-quark decay and to non-resonant effects, neither of which can be described by the MADSPIN procedure, and to off-shell effects, which MADSPIN can simulate only in an approximate manner. We thus conclude that, when targeting a less-than-10% accuracy, a better description of intermediate resonances is a necessity.

There are several aspects of this paper that will be interesting to consider in future work. The most obvious is the application of our findings to the matching of $t\bar{t}$ production with full off-shell effects ($W^+W^-b\bar{b}$) to parton showers. Furthermore, in view of the sometimes large differences between the PYTHIA8 and HERWIG6 predictions, it will also be worthwhile performing a careful study of the impact of shower initial conditions. This is because single-top production is an example of a multi-scale process for which a more sophisticated choice of shower scales might be required for an improved phenomenology treatment (as recently observed e.g. in ref. [71], which also deals with the presence of final-state b quarks). Finally, we point out that our results matched to the PYTHIA8 shower show qualitative agreement with those presented in ref. [45], which employ the POWHEG matching scheme. A thorough comparison of the two approaches using the same inputs and analysis setup would obviously be of great interest, and one which we intend to pursue.

Acknowledgments

A   Technicalities on the treatment of resonances

In this appendix we sketch the implementation in MADGRAPH5_AMC@NLO of the type-IIb solution alluded to in section 2.1.1, for the case of final-state singularities relevant to the FKS sector where the FKS pair belongs to the tree whose root is the resonance β. In order to simplify the discussion as much as possible, we shall proceed as in section 2.1, i.e. pretending that only soft singularities are present. However, as mentioned before, in MADGRAPH5_AMC@NLO all counterevents associated with a given event have the same reduced kinematics. Therefore, the actual formulae implemented in the program differ from those given below only by marginal technical aspects. We also recall that in the case of the singularities we are interested in, the phase-space parametrisation employed by MADGRAPH5_AMC@NLO is that of section 5.2 of ref. [28], and its generalisation to the case of a massive FKS sister. This implies that, using the labelling of figure 1:

$$k_\beta^2(b,\xi) = (k_\gamma + k_\mu)^2 \,, \qquad k_\beta^2(b,0) = \left(\bar{k}_\gamma + \bar{k}_\mu\right)^2 \,, \tag{A.1}$$

where the barred four-momenta $\bar{k}$ conventionally denote those of the counterevent configuration associated with the event configuration whose four-momenta are denoted by un-barred symbols k. Furthermore

$$\bar{k}_\gamma = \mathbb{B}\, k_\gamma \,, \qquad \bar{k}_\mu \neq \mathbb{B}\, k_\mu \,, \tag{A.2}$$

with $\mathbb{B}$ a boost. Therefore, eq. (2.3) is not fulfilled, whence the necessity of a type-II solution.

In order to proceed, let us start from the basic expression of the subtracted cross section, eq. (2.2), that we can replace with:

$$\int db \int_0^{\xi^{\mathrm{M}}(b)} d\xi \frac{1}{\xi} \left[\sigma\!\left(k_\beta^2(b,\xi)\,|\,b,\xi\right) - \sigma\!\left(k_\beta^2(b,0)\,|\,b,0\right) \right] \,, \tag{A.3}$$

where:

$$\varsigma(b,\xi) = \sigma(b,\xi)\Theta(\xi^{\mathrm{M}}(b) - \xi)\,. \tag{A.4}$$

Equation (A.3) differs from eq. (2.2) by a contribution due to the integral of the counterterm in the range $\xi > \xi^{\mathrm{M}}(b)$ (owing to the fact that for the soft counterterm the Θ function of eq. (A.4) is identically equal to one). As already discussed in section 2.1, Born-like terms do not pose significant problems in the presence of resonances. We shall thus ignore this contribution in what follows, and deal solely with eq. (A.3). In MADGRAPH5_AMC@NLO,

the parametrisation of Born-level integration variables in the context of an NLO computation is identical to that adopted for a tree-level computation of the same multiplicity (see ref. [52]). This implies that, by construction, one of the variables b will coincide with the virtuality of the resonance β, computed with the counterevent kinematics. Let us denote this variable by b_β, and all of the other integration variables collectively by $b_{\not\beta}$:

$$b = \{b_\beta, b_{\not\beta}\}.\qquad\qquad(\text{A.5})$$

By construction, one has:

$$b_\beta = k_\beta^2(b, 0) \equiv k_\beta^2(b_\beta, b_{\not\beta}, 0),\qquad\qquad(\text{A.6})$$

whereas, owing to eqs. (A.1) and (A.2):

$$b_\beta \neq k_\beta^2(b_\beta, b_{\not\beta}, \xi).\qquad\qquad(\text{A.7})$$

Equation (A.7) suggests that $k_\beta^2(b_\beta, b_{\not\beta}, \xi)$, seen as a function of b_β at fixed $(b_{\not\beta}, \xi)$, can be identified with Φ_ξ of eq. (2.5) for a one-dimensional change of integration variables for a type-IIa solution; its inverse can be used for a type-IIb solution.

We have considered both types of approaches, and found that the type-IIa one did not perform in a satisfactory manner from the numerical viewpoint. The reason is the following: with a type-IIa solution, both event and (re-mapped) counterevents have a Breit-Wigner peak at $k_\beta^2(b_\beta, b_{\not\beta}, \xi) \simeq m_\beta^2$. This implies that the integration variable b_β will *not* be peaked at m_β^2, but at a somewhat different (typically lower) value. Moreover, and more importantly, the position of such a peak will be correlated with the value of ξ (and, in the actual QCD case where collinear singularities are present, with that of the angle between the FKS parton and its sister). The first issue renders it difficult to guess analytically an efficient change of variables from the relevant "Vegas x" to b_β, which implies a longer-than-desired grid optimisation, while the second issue effectively hampers such an optimisation (since correlations are notoriously difficult to handle in adaptive integrations). For this reason, our solution of choice in MADGRAPH5_AMC@NLO is a type-IIb one, which we now proceed to describe in greater detail.

As discussed in section 2.1, type-IIb solutions entail the manipulation of the event contribution. We single out such contribution in eq. (A.3), which we implicitly and temporarily regularise (e.g. with a cutoff) in order to avoid divergences, and rewrite it as follows:

$$
\begin{aligned}
E &= \int db' \int_0^{\xi^{\mathrm{M}}(b')} \frac{d\xi}{\xi} \sigma\big(k_\beta^2(b', \xi)\,|\,b', \xi\big)\\
&\equiv \int db'_\beta db'_{\not\beta} \int_0^1 \frac{d\xi}{\xi} \sigma\Big(k_\beta^2(b'_\beta, b'_{\not\beta}, \xi)\,|\,b'_\beta, b'_{\not\beta}, \xi\Big)\,\Theta\Big(\xi^{\mathrm{M}}(b'_\beta, b'_{\not\beta}) - \xi\Big),
\end{aligned}
\qquad(\text{A.8})
$$

having trivially renamed b as b'. We then perform the following change of integration variables:

$$\{b'_\beta, b'_{\not\beta}\} \longrightarrow \{b_\beta, b_{\not\beta}\}, \qquad b'_{\not\beta} = b_{\not\beta}, \qquad b'_\beta = k_\beta^{2^{-1}}(b_\beta, b_{\not\beta}, \xi),\qquad(\text{A.9})$$

whence eq. (A.8) becomes:

$$E = \int db_\beta db_{\not\beta} \int_0^1 \frac{d\xi}{\xi} \frac{\partial k_\beta^{2^{-1}}(b_\beta, b_{\not\beta}, \xi)}{\partial b_\beta} \Theta\left(\xi^{\mathrm{M}}(k_\beta^{2^{-1}}(b_\beta, b_{\not\beta}, \xi), b_{\not\beta}) - \xi\right)$$
$$\times \sigma\left(b_\beta \mid k_\beta^{2^{-1}}(b_\beta, b_{\not\beta}, \xi), b_{\not\beta}, \xi\right). \quad (A.10)$$

The first argument of σ in eq. (A.10) shows that the event now has the desired property (thanks to eq. (A.6)), namely that the reconstructed invariant mass of the resonance is equal to that of the counterevent (generated with the same $\{b_\beta, b_{\not\beta}\}$ and not re-mapped), in keeping with the general derivation of type-IIb solutions. A drawback of eq. (A.10) is the possible difficulty of computing the jacobian analytically; in MADGRAPH5_AMC@NLO we bypassed this problem by resorting to entirely numerical methods (employing fast and readily available numerical-derivative routines, such as those of CERNLIB), with excellent performances in terms of stability and accuracy. The re-mapped subtracted cross section can finally be obtained by replacing the event contribution to eq. (A.3) with the r.h.s. of eq. (A.10). Such a form is essentially what is implemented in MADGRAPH5_AMC@NLO, barring numerically-small contributions due to the following features.

- The support of $k_\beta^2(b_\beta, b_{\not\beta}, \xi)$ is in general different w.r.t. that of its inverse. In this case, where either the event or the counterevents are equal to zero, no re-mapping is performed.

- It may happen that, for certain values of ξ (typically far from zero, and with a massive FKS sister) and close to the borders of the support of $k_\beta^2(b_\beta, b_{\not\beta}, \xi)$, such a function is not monotonic. Although one could carry out the procedure outlined above in a piece-wise manner, we have opted for not performing the re-mapping in such a case.

Finally, we point out that in our code the integration variable relevant to the FKS soft subtraction is not ξ, but actually its rescaled version $\hat{\xi}$, defined so that $\xi = \hat{\xi}\xi^{\mathrm{M}}(b)$. This guarantees a better numerical performance, chiefly owing to the complete absence of correlations between $\hat{\xi}$ and other integration variables.

Open Access. This article is distributed under the terms of the Creative Commons Attribution License (CC-BY 4.0), which permits any use, distribution and reproduction in any medium, provided the original author(s) and source are credited.

References

[1] CDF collaboration, T. Aaltonen et al., *First observation of electroweak single top quark production*, *Phys. Rev. Lett.* **103** (2009) 092002 [arXiv:0903.0885] [INSPIRE].

[2] D0 collaboration, V.M. Abazov et al., *Observation of single top quark production*, *Phys. Rev. Lett.* **103** (2009) 092001 [arXiv:0903.0850] [INSPIRE].

[3] CDF collaboration, T. Aaltonen et al., *Observation of single top quark production and measurement of $|V_{tb}|$ with CDF*, *Phys. Rev.* **D 82** (2010) 112005 [arXiv:1004.1181] [INSPIRE].

[4] D0 collaboration, V.M. Abazov et al., *Model-independent measurement of t-channel single top quark production in $p\bar{p}$ collisions at $\sqrt{s} = 1.96$ TeV*, *Phys. Lett.* **B 705** (2011) 313 [arXiv:1105.2788] [INSPIRE].

[5] CDF, D0 collaboration, T.A. Aaltonen et al., *Tevatron combination of single-top-quark cross sections and determination of the magnitude of the Cabibbo-Kobayashi-Maskawa matrix element V_{tb}*, *Phys. Rev. Lett.* **115** (2015) 152003 [arXiv:1503.05027] [INSPIRE].

[6] ATLAS collaboration, *Measurement of the t-channel single top-quark production cross section in pp collisions at $\sqrt{s} = 7$ TeV with the ATLAS detector*, *Phys. Lett.* **B 717** (2012) 330 [arXiv:1205.3130] [INSPIRE].

[7] ATLAS collaboration, *Comprehensive measurements of t-channel single top-quark production cross sections at $\sqrt{s} = 7$ TeV with the ATLAS detector*, *Phys. Rev.* **D 90** (2014) 112006 [arXiv:1406.7844] [INSPIRE].

[8] ATLAS collaboration, *Measurement of t-channel single top-quark production in pp collisions at $\sqrt{s} = 8$ TeV with the ATLAS detector*, ATLAS-CONF-2012-132 (2012).

[9] CMS collaboration, *Measurement of the t-channel single top quark production cross section in pp collisions at $\sqrt{s} = 7$ TeV*, *Phys. Rev. Lett.* **107** (2011) 091802 [arXiv:1106.3052] [INSPIRE].

[10] CMS collaboration, *Measurement of the single-top-quark t-channel cross section in pp collisions at $\sqrt{s} = 7$ TeV*, *JHEP* **12** (2012) 035 [arXiv:1209.4533] [INSPIRE].

[11] CMS collaboration, *Measurement of the t-channel single-top-quark production cross section and of the $|V_{tb}|$ CKM matrix element in pp collisions at $\sqrt{s} = 8$ TeV*, *JHEP* **06** (2014) 090 [arXiv:1403.7366] [INSPIRE].

[12] ATLAS collaboration, *Measurement of the inclusive cross-section of single top-quark t-channel production in pp collisions at $\sqrt{s} = 13$ TeV*, ATLAS-CONF-2015-079 (2015).

[13] CMS collaboration, *Measurement of the t-channel single top-quark cross section at 13 TeV*, CMS-PAS-TOP-15-004 (2015).

[14] ATLAS collaboration, *Measurement of the top quark mass in topologies enhanced with single top-quarks produced in the t-channel in $\sqrt{s} = 8$ TeV ATLAS data*, ATLAS-CONF-2014-055 (2014).

[15] CMS collaboration, *Evidence for associated production of a single top quark and W boson in pp collisions at $\sqrt{s} = 7$ TeV*, *Phys. Rev. Lett.* **110** (2013) 022003 [arXiv:1209.3489] [INSPIRE].

[16] CDF, D0 collaboration, T.A. Aaltonen et al., *Observation of s-channel production of single top quarks at the Tevatron*, *Phys. Rev. Lett.* **112** (2014) 231803 [arXiv:1402.5126] [INSPIRE].

[17] ATLAS collaboration, *Measurement of the production cross-section of a single top quark in association with a W boson at 8 TeV with the ATLAS experiment*, *JHEP* **01** (2016) 064 [arXiv:1510.03752] [INSPIRE].

[18] ATLAS collaboration, *Evidence for single top-quark production in the s-channel in proton-proton collisions at $\sqrt{s} = 8$ TeV with the ATLAS detector using the Matrix Element Method*, *Phys. Lett.* **B 756** (2016) 228 [arXiv:1511.05980] [INSPIRE].

[19] C. Zhang and S. Willenbrock, *Effective-field-theory approach to top-quark production and decay*, *Phys. Rev.* **D 83** (2011) 034006 [arXiv:1008.3869] [INSPIRE].

[20] Q.-H. Cao, B. Yan, J.-H. Yu and C. Zhang, *A general analysis of W_{tb} anomalous couplings*, arXiv:1504.03785 [INSPIRE].

[21] CMS collaboration, *Search for anomalous Wtb couplings and top FCNC in t-channel single-top-quark events*, CMS-PAS-TOP-14-007 (2014).

[22] ATLAS collaboration, *Search for anomalous couplings in the Wtb vertex from the measurement of double differential angular decay rates of single top quarks produced in the t-channel with the ATLAS detector*, JHEP **04** (2016) 023 [arXiv:1510.03764] [INSPIRE].

[23] S. Frixione, E. Laenen, P. Motylinski and B.R. Webber, *Single-top production in MC@NLO*, JHEP **03** (2006) 092 [hep-ph/0512250] [INSPIRE].

[24] S. Alioli, P. Nason, C. Oleari and E. Re, *NLO single-top production matched with shower in POWHEG: s- and t-channel contributions*, JHEP **09** (2009) 111 [*Erratum ibid.* **02** (2010) 011] [arXiv:0907.4076] [INSPIRE].

[25] R. Frederix, E. Re and P. Torrielli, *Single-top t-channel hadroproduction in the four-flavour scheme with POWHEG and aMC@NLO*, JHEP **09** (2012) 130 [arXiv:1207.5391] [INSPIRE].

[26] S. Frixione and B.R. Webber, *Matching NLO QCD computations and parton shower simulations*, JHEP **06** (2002) 029 [hep-ph/0204244] [INSPIRE].

[27] P. Nason, *A new method for combining NLO QCD with shower Monte Carlo algorithms*, JHEP **11** (2004) 040 [hep-ph/0409146] [INSPIRE].

[28] S. Frixione, P. Nason and C. Oleari, *Matching NLO QCD computations with Parton Shower simulations: the POWHEG method*, JHEP **11** (2007) 070 [arXiv:0709.2092] [INSPIRE].

[29] S. Frixione, E. Laenen, P. Motylinski and B.R. Webber, *Angular correlations of lepton pairs from vector boson and top quark decays in Monte Carlo simulations*, JHEP **04** (2007) 081 [hep-ph/0702198] [INSPIRE].

[30] M. Brucherseifer, F. Caola and K. Melnikov, *On the NNLO QCD corrections to single-top production at the LHC*, Phys. Lett. **B 736** (2014) 58 [arXiv:1404.7116] [INSPIRE].

[31] J.M. Campbell, R.K. Ellis and F. Tramontano, *Single top production and decay at next-to-leading order*, Phys. Rev. **D 70** (2004) 094012 [hep-ph/0408158] [INSPIRE].

[32] S. Heim, Q.-H. Cao, R. Schwienhorst and C.P. Yuan, *Next-to-leading order QCD corrections to s-channel single top quark production and decay at the LHC*, Phys. Rev. **D 81** (2010) 034005 [arXiv:0911.0620] [INSPIRE].

[33] R. Schwienhorst, C.P. Yuan, C. Mueller and Q.-H. Cao, *Single top quark production and decay in the t-channel at next-to-leading order at the LHC*, Phys. Rev. **D 83** (2011) 034019 [arXiv:1012.5132] [INSPIRE].

[34] J.M. Campbell and R.K. Ellis, *Top-quark processes at NLO in production and decay*, J. Phys. **G 42** (2015) 015005 [arXiv:1204.1513] [INSPIRE].

[35] P. Falgari, P. Mellor and A. Signer, *Production-decay interferences at NLO in QCD for t-channel single-top production*, Phys. Rev. **D 82** (2010) 054028 [arXiv:1007.0893] [INSPIRE].

[36] P. Falgari, F. Giannuzzi, P. Mellor and A. Signer, *Off-shell effects for t-channel and s-channel single-top production at NLO in QCD*, Phys. Rev. **D 83** (2011) 094013 [arXiv:1102.5267] [INSPIRE].

[37] A.S. Papanastasiou, R. Frederix, S. Frixione, V. Hirschi and F. Maltoni, *Single-top t-channel production with off-shell and non-resonant effects*, *Phys. Lett.* **B 726** (2013) 223 [arXiv:1305.7088] [INSPIRE].

[38] A. Denner, S. Dittmaier, M. Roth and D. Wackeroth, *Predictions for all processes $e^+e^- \to 4$ fermions + gamma*, *Nucl. Phys.* **B 560** (1999) 33 [hep-ph/9904472] [INSPIRE].

[39] A. Denner, S. Dittmaier, M. Roth and L.H. Wieders, *Electroweak corrections to charged-current $e^+e^- \to 4$ fermion processes: technical details and further results*, *Nucl. Phys.* **B 724** (2005) 247 [*Erratum ibid.* **B 854** (2012) 504] [hep-ph/0505042] [INSPIRE].

[40] K. Melnikov and M. Schulze, *NLO QCD corrections to top quark pair production and decay at hadron colliders*, *JHEP* **08** (2009) 049 [arXiv:0907.3090] [INSPIRE].

[41] A. Denner, S. Dittmaier, S. Kallweit and S. Pozzorini, *NLO QCD corrections to WWbb production at hadron colliders*, *Phys. Rev. Lett.* **106** (2011) 052001 [arXiv:1012.3975] [INSPIRE].

[42] SM MC WORKING GROUP, SM AND NLO MULTILEG WORKING GROUP collaboration, J. Alcaraz Maestre et al., *The SM and NLO multileg and SM MC working groups: summary report*, arXiv:1203.6803 [INSPIRE].

[43] P. Falgari, A.S. Papanastasiou and A. Signer, *Finite-width effects in unstable-particle production at hadron colliders*, *JHEP* **05** (2013) 156 [arXiv:1303.5299] [INSPIRE].

[44] J.M. Campbell, R.K. Ellis, P. Nason and E. Re, *Top-pair production and decay at NLO matched with parton showers*, *JHEP* **04** (2015) 114 [arXiv:1412.1828] [INSPIRE].

[45] T. Ježo and P. Nason, *On the treatment of resonances in next-to-leading order calculations matched to a parton shower*, *JHEP* **12** (2015) 065 [arXiv:1509.09071] [INSPIRE].

[46] G. Corcella et al., *HERWIG 6: an event generator for hadron emission reactions with interfering gluons (including supersymmetric processes)*, *JHEP* **01** (2001) 010 [hep-ph/0011363] [INSPIRE].

[47] G. Corcella et al., *HERWIG 6.5 release note*, hep-ph/0210213 [INSPIRE].

[48] T. Sjöstrand, S. Mrenna and P.Z. Skands, *A brief introduction to PYTHIA 8.1*, *Comput. Phys. Commun.* **178** (2008) 852 [arXiv:0710.3820] [INSPIRE].

[49] J. Alwall et al., *The automated computation of tree-level and next-to-leading order differential cross sections and their matching to parton shower simulations*, *JHEP* **07** (2014) 079 [arXiv:1405.0301] [INSPIRE].

[50] S. Frixione, Z. Kunszt and A. Signer, *Three jet cross-sections to next-to-leading order*, *Nucl. Phys.* **B 467** (1996) 399 [hep-ph/9512328] [INSPIRE].

[51] S. Frixione, *A general approach to jet cross-sections in QCD*, *Nucl. Phys.* **B 507** (1997) 295 [hep-ph/9706545] [INSPIRE].

[52] R. Frederix, S. Frixione, F. Maltoni and T. Stelzer, *Automation of next-to-leading order computations in QCD: the FKS subtraction*, *JHEP* **10** (2009) 003 [arXiv:0908.4272] [INSPIRE].

[53] G. Ossola, C.G. Papadopoulos and R. Pittau, *Reducing full one-loop amplitudes to scalar integrals at the integrand level*, *Nucl. Phys.* **B 763** (2007) 147 [hep-ph/0609007] [INSPIRE].

[54] G. Passarino and M.J.G. Veltman, *One loop corrections for e^+e^- annihilation into $\mu^+\mu^-$ in the Weinberg model*, *Nucl. Phys.* **B 160** (1979) 151 [INSPIRE].

[55] A.I. Davydychev, *A simple formula for reducing Feynman diagrams to scalar integrals*, *Phys. Lett.* **B 263** (1991) 107 [INSPIRE].

[56] A. Denner and S. Dittmaier, *Reduction schemes for one-loop tensor integrals*, *Nucl. Phys.* **B 734** (2006) 62 [hep-ph/0509141] [INSPIRE].

[57] V. Hirschi, R. Frederix, S. Frixione, M.V. Garzelli, F. Maltoni and R. Pittau, *Automation of one-loop QCD corrections*, *JHEP* **05** (2011) 044 [arXiv:1103.0621] [INSPIRE].

[58] G. Ossola, C.G. Papadopoulos and R. Pittau, *CutTools: a program implementing the OPP reduction method to compute one-loop amplitudes*, *JHEP* **03** (2008) 042 [arXiv:0711.3596] [INSPIRE].

[59] F. Cascioli, P. Maierhofer and S. Pozzorini, *Scattering amplitudes with open loops*, *Phys. Rev. Lett.* **108** (2012) 111601 [arXiv:1111.5206] [INSPIRE].

[60] F. Maltoni and T. Stelzer, *MadEvent: automatic event generation with MadGraph*, *JHEP* **02** (2003) 027 [hep-ph/0208156] [INSPIRE].

[61] G. Bevilacqua, M. Czakon, A. van Hameren, C.G. Papadopoulos and M. Worek, *Complete off-shell effects in top quark pair hadroproduction with leptonic decay at next-to-leading order*, *JHEP* **02** (2011) 083 [arXiv:1012.4230] [INSPIRE].

[62] A. Denner, S. Dittmaier, S. Kallweit and S. Pozzorini, *NLO QCD corrections to off-shell top-antitop production with leptonic decays at hadron colliders*, *JHEP* **10** (2012) 110 [arXiv:1207.5018] [INSPIRE].

[63] R. Frederix, *Top quark induced backgrounds to Higgs production in the $WW^{(*)} \to ll\nu\nu$ decay channel at next-to-leading-order in QCD*, *Phys. Rev. Lett.* **112** (2014) 082002 [arXiv:1311.4893] [INSPIRE].

[64] F. Cascioli, S. Kallweit, P. Maierhöfer and S. Pozzorini, *A unified NLO description of top-pair and associated Wt production*, *Eur. Phys. J.* **C 74** (2014) 2783 [arXiv:1312.0546] [INSPIRE].

[65] G. Heinrich, A. Maier, R. Nisius, J. Schlenk and J. Winter, *NLO QCD corrections to $W^+W^-b\bar{b}$ production with leptonic decays in the light of top quark mass and asymmetry measurements*, *JHEP* **06** (2014) 158 [arXiv:1312.6659] [INSPIRE].

[66] S. Catani, Y.L. Dokshitzer, M.H. Seymour and B.R. Webber, *Longitudinally invariant K_t clustering algorithms for hadron hadron collisions*, *Nucl. Phys.* **B 406** (1993) 187 [INSPIRE].

[67] M. Cacciari, G.P. Salam and G. Soyez, *FastJet user manual*, *Eur. Phys. J.* **C 72** (2012) 1896 [arXiv:1111.6097] [INSPIRE].

[68] P. Artoisenet, R. Frederix, O. Mattelaer and R. Rietkerk, *Automatic spin-entangled decays of heavy resonances in Monte Carlo simulations*, *JHEP* **03** (2013) 015 [arXiv:1212.3460] [INSPIRE].

[69] R. Frederix, S. Frixione, V. Hirschi, F. Maltoni, R. Pittau and P. Torrielli, *Four-lepton production at hadron colliders: aMC@NLO predictions with theoretical uncertainties*, *JHEP* **02** (2012) 099 [arXiv:1110.4738] [INSPIRE].

[70] A.D. Martin, W.J. Stirling, R.S. Thorne and G. Watt, *Parton distributions for the LHC*, *Eur. Phys. J.* **C 63** (2009) 189 [arXiv:0901.0002] [INSPIRE].

[71] M. Wiesemann et al., *Higgs production in association with bottom quarks*, *JHEP* **02** (2015) 132 [arXiv:1409.5301] [INSPIRE].